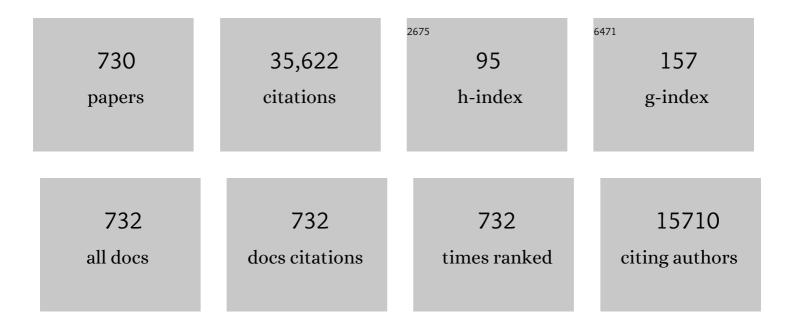
David J Richardson

List of Publications by Year in descending order

Source: https://exaly.com/author-pdf/6104686/publications.pdf Version: 2024-02-01



#	Article	IF	CITATIONS
1	Space-division multiplexing in optical fibres. Nature Photonics, 2013, 7, 354-362.	31.4	2,606
2	All-optical phase and amplitude regenerator for next-generation telecommunications systems. Nature Photonics, 2010, 4, 690-695.	31.4	595
3	Bacterial respiration: a flexible process for a changing environment 1999 Fleming Lecture (Delivered) Tj ETQq1 1	0.784314 1.8	rgBT /Overlo 508
4	Hexagonally Poled Lithium Niobate: A Two-Dimensional Nonlinear Photonic Crystal. Physical Review Letters, 2000, 84, 4345-4348.	7.8	468
5	Ultra-low-loss optical fiber nanotapers. Optics Express, 2004, 12, 2258.	3.4	445
6	Mitigating release of the potent greenhouse gas N2O from the nitrogen cycle – could enzymic regulation hold the key?. Trends in Biotechnology, 2009, 27, 388-397.	9.3	438
7	Selfstarting passively mode-locked fibre ring soliton laser exploiting nonlinear polarisation rotation. Electronics Letters, 1992, 28, 1391.	1.0	432
8	Characterization of an electron conduit between bacteria and the extracellular environment. Proceedings of the National Academy of Sciences of the United States of America, 2009, 106, 22169-22174.	7.1	410
9	Roadmap of optical communications. Journal of Optics (United Kingdom), 2016, 18, 063002.	2.2	402
10	Sensing with microstructured optical fibres. Measurement Science and Technology, 2001, 12, 854-858.	2.6	351
11	Holey optical fibers: an efficient modal model. Journal of Lightwave Technology, 1999, 17, 1093-1102.	4.6	343
12	Self-similarity in ultrafast nonlinear optics. Nature Physics, 2007, 3, 597-603.	16.7	336
13	Optical fiber nanowires and microwires: fabrication and applications. Advances in Optics and Photonics, 2009, 1, 107.	25.5	311
14	Filling the Light Pipe. Science, 2010, 330, 327-328.	12.6	303
15	Structure of a bacterial cell surface decaheme electron conduit. Proceedings of the National Academy of Sciences of the United States of America, 2011, 108, 9384-9389.	7.1	301
16	Nonlinearity in holey optical fibers: measurement and future opportunities. Optics Letters, 1999, 24, 1395.	3.3	295
17	Towards high-capacity fibre-optic communications at the speed of light in vacuum. Nature Photonics, 2013, 7, 279-284.	31.4	289
18	The roles of outer membrane cytochromes of <i>Shewanella</i> and <i>Geobacter</i> in extracellular electron transfer. Environmental Microbiology Reports, 2009, 1, 220-227.	2.4	285

#	Article	IF	CITATIONS
19	Thulium-doped fiber amplifier for optical communications at 2 µm. Optics Express, 2013, 21, 9289.	3.4	266
20	Passively Q-switched 01-mJ fiber laser system at 153 ?m. Optics Letters, 1999, 24, 388.	3.3	225
21	Energy quantisation in figure eight fibre laser. Electronics Letters, 1992, 28, 67-68.	1.0	223
22	The â€~porin–cytochrome' model for microbeâ€toâ€mineral electron transfer. Molecular Microbiology, 2012, 85, 201-212.	2.5	222
23	Periplasmic and membrane-bound respiratory nitrate reductases inThiosphaera pantotropha. FEBS Letters, 1990, 265, 85-87.	2.8	219
24	Enhancing optical communications with brand new fibers. , 2012, 50, s31-s42.		210
25	Characterization of the Shewanella oneidensis MR-1 Decaheme Cytochrome MtrA. Journal of Biological Chemistry, 2003, 278, 27758-27765.	3.4	209
26	Characterization of Shewanella oneidensis MtrC: a cell-surface decaheme cytochrome involved in respiratory electron transport to extracellular electron acceptors. Journal of Biological Inorganic Chemistry, 2007, 12, 1083-1094.	2.6	209
27	Soliton pulse compression in dispersion-decreasing fiber. Optics Letters, 1993, 18, 476.	3.3	204
28	Interrogation of fiber grating sensor arrays with a wavelength-swept fiber laser. Optics Letters, 1998, 23, 843.	3.3	204
29	Architecture of NarGH Reveals a Structural Classification of Mo-bisMGD Enzymes. Structure, 2004, 12, 95-104.	3.3	199
30	Chalcogenide holey fibres. Electronics Letters, 2000, 36, 1998.	1.0	198
31	Molecular Underpinnings of Fe(III) Oxide Reduction by Shewanella Oneidensis MR-1. Frontiers in Microbiology, 2012, 3, 50.	3.5	186
32	Mid-IR Supercontinuum Generation From Nonsilica Microstructured Optical Fibers. IEEE Journal of Selected Topics in Quantum Electronics, 2007, 13, 738-749.	2.9	181
33	Rapid electron exchange between surface-exposed bacterial cytochromes and Fe(III) minerals. Proceedings of the National Academy of Sciences of the United States of America, 2013, 110, 6346-6351.	7.1	179
34	Modeling large air fraction holey optical fibers. Journal of Lightwave Technology, 2000, 18, 50-56.	4.6	178
35	A transâ€outer membrane porinâ€cytochrome protein complex for extracellular electron transfer by <scp><i>G</i></scp> <i>eobacter sulfurreducens</i> â€ <scp>PCA</scp> . Environmental Microbiology Reports, 2014, 6, 776-785.	2.4	178
36	First demonstration and detailed characterization of a multimode amplifier for space division multiplexed transmission systems. Optics Express, 2011, 19, B952.	3.4	174

#	Article	IF	CITATIONS
37	High-energy, high-power ytterbium-doped Q-switched fiber laser. Optics Letters, 2000, 25, 37.	3.3	172
38	320 fs soliton generation with passively mode-locked erbium fibre laser. Electronics Letters, 1991, 27, 730.	1.0	171
39	Respiratory Detoxification of Nitric Oxide by the Cytochromec Nitrite Reductase of Escherichia coli. Journal of Biological Chemistry, 2002, 277, 23664-23669.	3.4	171
40	Bacterial Adaptation of Respiration from Oxic to Microoxic and Anoxic Conditions: Redox Control. Antioxidants and Redox Signaling, 2012, 16, 819-852.	5.4	170
41	Hollow-core photonic bandgap fibers: technology and applications. Nanophotonics, 2013, 2, 315-340.	6.0	170
42	Ultra-flat SPM-broadened spectra in a highly nonlinear fiber using parabolic pulses formed in a fiber Bragg grating. Optics Express, 2006, 14, 7617.	3.4	167
43	Selfstarting, passively modelocked erbium fibre ring laser based on the amplifying Sagnac switch. Electronics Letters, 1991, 27, 542.	1.0	165
44	Cladding pumped Ytterbium-doped fiber laser with holey inner and outer cladding. Optics Express, 2001, 9, 714.	3.4	165
45	Highly nonlinear and anomalously dispersive lead silicate glass holey fibers. Optics Express, 2003, 11, 3568.	3.4	165
46	Diode-pumped wideband thulium-doped fiber amplifiers for optical communications in the 1800 – 2050 nm window. Optics Express, 2013, 21, 26450.	3.4	165
47	A comparative study of the performance of seven- and 63-chip optical code-division multiple-access encoders and decoders based on superstructured fiber Bragg gratings. Journal of Lightwave Technology, 2001, 19, 1352-1365.	4.6	159
48	158-µJ pulses from a single-transverse-mode, large-mode-area erbium-doped fiber amplifier. Optics Letters, 1997, 22, 378.	3.3	157
49	737 Tb/s (96 x 3 x 256-Gb/s) mode-division-multiplexed DP-16QAM transmission with inline MM-EDFA. Optics Express, 2012, 20, B428.	3.4	156
50	Toward practical holey fiber technology:?fabrication, splicing, modeling, and characterization. Optics Letters, 1999, 24, 1203.	3.3	153
51	Nonlinear self-switching and multiple gap-soliton formation in a fiber Bragg grating. Optics Letters, 1998, 23, 328.	3.3	152
52	Structure and Spectroscopy of the Periplasmic Cytochrome <i>c</i> Nitrite Reductase from <i>Escherichia coli</i> . Biochemistry, 2002, 41, 2921-2931.	2.5	151
53	Extruded singlemode non-silica glass holey optical fibres. Electronics Letters, 2002, 38, 546.	1.0	149
54	Characterization of Protein-Protein Interactions Involved in Iron Reduction by <i>Shewanella oneidensis</i> MR-1. Applied and Environmental Microbiology, 2007, 73, 5797-5808.	3.1	145

#	Article	IF	CITATIONS
55	Multilevel quantization of optical phase in a novel coherent parametric mixer architecture. Nature Photonics, 2011, 5, 748-752.	31.4	145
56	Sequence analysis of subunits of the membrane-bound nitrate reductase from a denitrifying bacterium: the integral membrane subunit provides a prototype for the dihaem electron-carrying arm of a redox loop. Molecular Microbiology, 1995, 15, 319-331.	2.5	144
57	Propagation of Cold Atoms along a Miniature Magnetic Guide. Physical Review Letters, 2000, 84, 1371-1373.	7.8	144
58	Optical manipulation of microspheres along a subwavelength optical wire. Optics Letters, 2007, 32, 3041.	3.3	144
59	Developing holey fibres for evanescent field devices. Electronics Letters, 1999, 35, 1188.	1.0	142
60	Rectangular pulse generation based on pulse reshaping using a superstructured fiber Bragg grating. Journal of Lightwave Technology, 2001, 19, 746-752.	4.6	142
61	Single-mode tellurite glass holey fiber with extremely large mode area for infrared nonlinear applications. Optics Express, 2008, 16, 13651.	3.4	140
62	Redox Linked Flavin Sites in Extracellular Decaheme Proteins Involved in Microbe-Mineral Electron Transfer Scientific Reports, 2015, 5, 11677.	3.3	138
63	Supercontinuum generation at 1.06 \hat{l} ¹ /4m in holey fibers with dispersion flattened profiles. Optics Express, 2006, 14, 4445.	3.4	137
64	2R-regenerative all-optical switch based on a highly nonlinear holey fiber. Optics Letters, 2001, 26, 1233.	3.3	135
65	Nonlinear femtosecond pulse compression at high average power levels by use of a large-mode-area holey fiber. Optics Letters, 2003, 28, 1951.	3.3	131
66	Spectroscopic Characterization of a Novel Multihemec-Type Cytochrome Widely Implicated in Bacterial Electron Transport. Journal of Biological Chemistry, 1998, 273, 28785-28790.	3.4	129
67	Small-core silica holey fibers: nonlinearity and confinement loss trade-offs. Journal of the Optical Society of America B: Optical Physics, 2003, 20, 1427.	2.1	128
68	Nitrate reduction in the periplasm of gram-negative bacteria. Advances in Microbial Physiology, 2001, 45, 51-112.	2.4	126
69	High-energy single-transverse-mode Q-switched fiber laser based on a multimode large-mode-area erbium-doped fiber. Optics Letters, 1998, 23, 1683.	3.3	124
70	Large Mode Area Fibers for High Power Applications. Optical Fiber Technology, 1999, 5, 185-196.	2.7	124
71	Characteristics of Q-switched cladding-pumped ytterbium-doped fiber lasers with different high-energy fiber designs. IEEE Journal of Quantum Electronics, 2001, 37, 199-206.	1.9	121
72	Holey fibers with random cladding distributions. Optics Letters, 2000, 25, 206.	3.3	120

#	Article	IF	CITATIONS
73	High-nonlinearity dispersion-shifted lead-silicate holey fibers for efficient 1-/spl mu/m pumped supercontinuum generation. Journal of Lightwave Technology, 2006, 24, 183-190.	4.6	120
74	Micro-channels machined in microstructured optical fibers by femtosecond laser. Optics Express, 2007, 15, 8731.	3.4	118
75	High power pulsed fiber MOPA system incorporating electro-optic modulator based adaptive pulse shaping. Optics Express, 2009, 17, 20927.	3.4	117
76	The purification of a cd1-type nitrite reductase from, and the absence of a copper-type nitrite reductase from, the aerobic denitrifier Thiosphaera pantotropha; the role of pseudoazurin as an electron donor. FEBS Journal, 1993, 212, 377-385.	0.2	116
77	Characterization of a self-starting, passively mode-locked fiber ring laser that exploits nonlinear polarization evolution. Optics Letters, 1993, 18, 358.	3.3	115
78	Catalytic Protein Film Voltammetry from a Respiratory Nitrate Reductase Provides Evidence for Complex Electrochemical Modulation of Enzyme Activityâ€. Biochemistry, 2001, 40, 11294-11307.	2.5	115
79	Compound-glass optical nanowires. Electronics Letters, 2005, 41, 400.	1.0	114
80	Picosecond fiber MOPA pumped supercontinuum source with 39 W output power. Optics Express, 2010, 18, 5426.	3.4	113
81	Noise suppression of incoherent light using a gain-saturated SOA: implications for spectrum-sliced WDM systems. Journal of Lightwave Technology, 2005, 23, 2399-2409.	4.6	112
82	Demonstration of amplified data transmission at 2 µm in a low-loss wide bandwidth hollow core photonic bandgap fiber. Optics Express, 2013, 21, 28559.	3.4	112
83	100 Gbit/s WDM transmission at 2 µm: transmission studies in both low-loss hollow core photonic bandgap fiber and solid core fiber. Optics Express, 2015, 23, 4946.	3.4	111
84	Si-rich Silicon Nitride for Nonlinear Signal Processing Applications. Scientific Reports, 2017, 7, 22.	3.3	111
85	Four-wave mixing based 10-Gb/s tunable wavelength conversion using a holey fiber with a high SBS threshold. IEEE Photonics Technology Letters, 2003, 15, 440-442.	2.5	110
86	High average power, high repetition rate, picosecond pulsed fiber master oscillator power amplifier source seeded by a gain-switched laser diode at 1060 nm. IEEE Photonics Technology Letters, 2006, 18, 1013-1015.	2.5	109
87	Look on the positive side! The orientation, identification and bioenergetics of â€Â [~] Archaeal' membrane-bound nitrate reductases. FEMS Microbiology Letters, 2007, 276, 129-139.	1.8	107
88	Demonstration of Berry's Phase Using Stored Ultracold Neutrons. Physical Review Letters, 1988, 61, 2030-2033.	7.8	105
89	Purification and Magneto-optical Spectroscopic Characterization of Cytoplasmic Membrane and Outer Membrane Multiheme c-Type Cytochromes from Shewanella frigidimarina NCIMB400. Journal of Biological Chemistry, 2000, 275, 8515-8522.	3.4	105
90	Optical microfiber coupler for broadband single-mode operation. Optics Express, 2009, 17, 5273.	3.4	105

#	Article	IF	CITATIONS
91	Nonlinear propagation effects in an AlGaAs Bragg grating filter. Optics Letters, 1999, 24, 685.	3.3	104
92	Generation of a 40-GHz pulse stream by pulse multiplication with a sampled fiber Bragg grating. Optics Letters, 2000, 25, 521.	3.3	103
93	Cladding pumped few-mode EDFA for mode division multiplexed transmission. Optics Express, 2014, 22, 29008.	3.4	103
94	Greater than 20%-efficient frequency doubling of 1532-nm nanosecond pulses in quasi-phase-matched germanosilicate optical fibers. Optics Letters, 1999, 24, 208.	3.3	102
95	Parabolic pulse generation through passive nonlinear pulse reshaping in a normally dispersive two segment fiber device. Optics Express, 2007, 15, 852.	3.4	102
96	Parabolic pulse evolution in normally dispersive fiber amplifiers preceding the similariton formation regime. Optics Express, 2006, 14, 3161.	3.4	100
97	Models for Molybdenum Coordination during the Catalytic Cycle of Periplasmic Nitrate Reductase from Paracoccus denitrificans Derived from EPR and EXAFS Spectroscopy. Biochemistry, 1999, 38, 9000-9012.	2.5	99
98	The Nitric Oxide Reductase Activity of Cytochrome c Nitrite Reductase from Escherichia coli. Journal of Biological Chemistry, 2008, 283, 9587-9594.	3.4	97
99	Antiresonant Hollow Core Fiber With an Octave Spanning Bandwidth for Short Haul Data Communications. Journal of Lightwave Technology, 2017, 35, 437-442.	4.6	96
100	Fiber LPG Mode Converters and Mode Selection Technique for Multimode SDM. IEEE Photonics Technology Letters, 2012, 24, 1922-1925.	2.5	95
101	Understanding bending losses in holey optical fibers. Optics Communications, 2003, 227, 317-335.	2.1	94
102	Spectropotentiometric and Structural Analysis of the Periplasmic Nitrate Reductase from Escherichia coli. Journal of Biological Chemistry, 2007, 282, 6425-6437.	3.4	94
103	Design scaling rules for 2R-optical self-phase modulation-based regenerators. Optics Express, 2007, 15, 5100.	3.4	94
104	High-power, high repetition rate picosecond and femtosecond sources based on Yb-doped fiber amplification of VECSELs. Optics Express, 2006, 14, 9611.	3.4	93
105	Robustly single mode hollow core photonic bandgap fiber. Optics Express, 2008, 16, 4337.	3.4	92
106	Broadband single-mode operation of standard optical fibers by using a sub-wavelength optical wire filter. Optics Express, 2008, 16, 14661.	3.4	92
107	Constraining the conditions conducive to dissimilatory nitrate reduction to ammonium in temperate arable soils. Soil Biology and Biochemistry, 2011, 43, 1607-1611.	8.8	92
108	Adaptive pulse shape control in a diode-seeded nanosecond fiber MOPA system. Optics Express, 2006, 14, 10996.	3.4	91

#	Article	IF	CITATIONS
109	High-resolution microwave frequency transfer over an 86-km-long optical fiber network using a mode-locked laser. Optics Letters, 2011, 36, 511.	3.3	91
110	Accurate modal gain control in a multimode erbium doped fiber amplifier incorporating ring doping and a simple LP_01 pump configuration. Optics Express, 2012, 20, 20835.	3.4	91
111	The mathematical modelling of capillary drawing for holey fibre manufacture. Journal of Engineering Mathematics, 2002, 43, 201-227.	1.2	90
112	Optical Parabolic Pulse Generation and Applications. IEEE Journal of Quantum Electronics, 2009, 45, 1482-1489.	1.9	89
113	Supercontinuum generation in non-silica fibers. Optical Fiber Technology, 2012, 18, 327-344.	2.7	89
114	Pulse repetition rates in passive, selfstarting, femtosecond soliton fibre laser. Electronics Letters, 1991, 27, 1451.	1.0	88
115	Raman effects in a highly nonlinear holey fiber: amplification and modulation. Optics Letters, 2002, 27, 424.	3.3	88
116	Optimizing the usable bandwidth and loss through core design in realistic hollow-core photonic bandgap fibers. Optics Express, 2006, 14, 7974.	3.4	88
117	Resolution of Distinct Membrane-Bound Enzymes from Enterobacter cloacae SLD1a-1 That Are Responsible for Selective Reduction of Nitrate and Selenate Oxyanions. Applied and Environmental Microbiology, 2006, 72, 5173-5180.	3.1	88
118	Protein Film Voltammetry Reveals Distinctive Fingerprints of Nitrite and Hydroxylamine Reduction by a Cytochrome c Nitrite Reductase. Journal of Biological Chemistry, 2002, 277, 23374-23381.	3.4	87
119	Intensity measurement bend sensors based on periodically tapered soft glass fibers. Optics Letters, 2011, 36, 558.	3.3	87
120	Demonstration of a four-channel WDM/OCDMA system using 255-chip 320-Gchip/s quarternary phase coding gratings. IEEE Photonics Technology Letters, 2002, 14, 227-229.	2.5	86
121	Stretched pulse Yb^3+:silica fiber laser. Optics Letters, 1997, 22, 316.	3.3	84
122	Signal peptide–chaperone interactions on the twin-arginine protein transport pathway. Proceedings of the National Academy of Sciences of the United States of America, 2005, 102, 8460-8465.	7.1	84
123	Mid-infrared ZBLAN fiber supercontinuum source using picosecond diode-pumping at 2 µm. Optics Express, 2013, 21, 24281.	3.4	83
124	NapGH components of the periplasmic nitrate reductase of Escherichia coli K-12: location, topology and physiological roles in quinol oxidation and redox balancing. Biochemical Journal, 2004, 379, 47-55.	3.7	80
125	Phase sensitive amplification based on quadratic cascading in a periodically poled lithium niobate waveguide. Optics Express, 2009, 17, 20393.	3.4	80
126	All-fiber, ultra-wideband tunable laser at $2\hat{A}^{1}$ /4m. Optics Letters, 2013, 38, 4739.	3.3	80

#	Article	IF	CITATIONS
127	A holey fiber-based nonlinear thresholding device for optical CDMA receiver performance enhancement. IEEE Photonics Technology Letters, 2002, 14, 876-878.	2.5	78
128	Broadband high birefringence and polarizing hollow core antiresonant fibers. Optics Express, 2016, 24, 22943.	3.4	78
129	Purification and characterization of a nitrous oxide reductase from Thiosphaera pantotropha. Implications for the mechanism of aerobic nitrous oxide reduction. FEBS Journal, 1993, 212, 467-476.	0.2	77
130	Open conformation of a flavocytochrome c3 fumarate reductase. Nature Structural Biology, 1999, 6, 1104-1107.	9.7	77
131	All-optical and gate based on coupled gap-soliton formation in a fiber Bragg grating. Optics Letters, 1998, 23, 259.	3.3	76
132	Ultrashort-pulse Yb^3+-fiber-based laser and amplifier system producing >25-W average power. Optics Letters, 2004, 29, 2073.	3.3	76
133	Ultralow thermal sensitivity of phase and propagation delay in hollow core optical fibres. Scientific Reports, 2015, 5, 15447.	3.3	75
134	High Capacity Mode-Division Multiplexed Optical Transmission in a Novel 37-cell Hollow-Core Photonic Bandgap Fiber. Journal of Lightwave Technology, 2014, 32, 854-863.	4.6	74
135	Reconfigurable Modal Gain Control of a Few-Mode EDFA Supporting Six Spatial Modes. IEEE Photonics Technology Letters, 2014, 26, 1100-1103.	2.5	74
136	Comparative study of large-mode holey and conventional fibers. Optics Letters, 2001, 26, 1045.	3.3	73
137	Soliton transmission and supercontinuum generation in holey fiber, using a diode pumped Ytterbium fiber source. Optics Express, 2002, 10, 382.	3.4	73
138	Tuning a Nitrate Reductase for Function. Journal of Biological Chemistry, 2004, 279, 32212-32218.	3.4	73
139	The Xâ€ray crystal structure of <i>Shewanella oneidensis</i> OmcA reveals new insight at the microbe–mineral interface. FEBS Letters, 2014, 588, 1886-1890.	2.8	73
140	Fibre-optic metadevice for all-optical signal modulation based on coherent absorption. Nature Communications, 2018, 9, 182.	12.8	73
141	The effect of core asymmetries on the polarization properties of hollow core photonic bandgap fibers. Optics Express, 2005, 13, 9115.	3.4	71
142	Structural diversity in twin-arginine signal peptide-binding proteins. Proceedings of the National Academy of Sciences of the United States of America, 2007, 104, 15641-15646.	7.1	71
143	Dissemination of an optical frequency comb over fiber with 3 × 10^â^'18 fractional accuracy. Optics Express, 2012, 20, 1775.	3.4	69
144	Evaluating two concepts for the modelling of intermediates accumulation during biological denitrification in wastewater treatment. Water Research, 2015, 71, 21-31.	11.3	69

#	Article	IF	CITATIONS
145	Low-Loss 25.3 km Few-Mode Ring-Core Fiber for Mode-Division Multiplexed Transmission. Journal of Lightwave Technology, 2017, 35, 1363-1368.	4.6	69
146	Hollow Core NANF with 0.28 dB/km Attenuation in the C and L Bands. , 2020, , .		69
147	Picosecond soliton pulse compressor based on dispersion decreasing fibre. Electronics Letters, 1992, 28, 1842.	1.0	68
148	Practical low-noise stretched-pulse Yb^3+-doped fiber laser. Optics Letters, 2002, 27, 291.	3.3	68
149	Extruded singlemode, high-nonlinearity, tellurite glass holey fibre. Electronics Letters, 2005, 41, 835.	1.0	68
150	Pulse retiming based on XPM using parabolic pulses formed in a fiber Bragg grating. IEEE Photonics Technology Letters, 2006, 18, 829-831.	2.5	68
151	A 103 W erbium–ytterbium co-doped large-core fiber laser. Optics Communications, 2003, 227, 159-163.	2.1	67
152	Temperature and wavelength tuning of second-, third-, and fourth-harmonic generation in a two-dimensional hexagonally poled nonlinear crystal. Journal of the Optical Society of America B: Optical Physics, 2002, 19, 2263.	2.1	66
153	Detailed characterization of aâ€`fiber-optic parametric amplifier in phase-sensitive and phase-insensitive operation. Optics Express, 2010, 18, 4130.	3.4	66
154	114 Gbit/s soliton train generation through Raman selfâ€scattering of a dual frequency beat signal in dispersion decreasing optical fiber. Applied Physics Letters, 1993, 63, 293-295.	3.3	65
155	Low-loss and low-bend-sensitivity mid-infrared guidance in a hollow-core–photonic-bandgap fiber. Optics Letters, 2014, 39, 295.	3.3	65
156	High-Capacity Directly Modulated Optical Transmitter for 2-μm Spectral Region. Journal of Lightwave Technology, 2015, 33, 1373-1379.	4.6	65
157	0.174 dB/km Hollow Core Double Nested Antiresonant Nodeless Fiber (DNANF). , 2022, , .		65
158	Nitrous oxide production in soil isolates of nitrateâ€ e mmonifying bacteria. Environmental Microbiology Reports, 2012, 4, 66-71.	2.4	64
159	Multi-kilometer Long, Longitudinally Uniform Hollow Core Photonic Bandgap Fibers for Broadband Low Latency Data Transmission. Journal of Lightwave Technology, 2016, 34, 104-113.	4.6	64
160	Characterization of a flavocytochrome that is induced during the anaerobic respiration of Fe3+ by Shewanella frigidimarina NCIMB400. Biochemical Journal, 1999, 342, 439-448.	3.7	63
161	Generation of localized pulses from incoherent wave in optical fiber lines made of concatenated Mamyshev regenerators. Journal of the Optical Society of America B: Optical Physics, 2008, 25, 1537.	2.1	63
162	Experimental demonstration of 100 GHz dark soliton generation and propagation using a dispersion decreasing fibre. Electronics Letters, 1994, 30, 1326-1327.	1.0	62

#	Article	IF	CITATIONS
163	Optical Pulse Compression in Fiber Bragg Gratings. Physical Review Letters, 1997, 79, 4566-4569.	7.8	62
164	Polarisation maintaining 100W Yb-fiber †MOPA producing µJ pulses tunable in †duration from 1 to 21 ps. Optics Express, 2010, 18, 14385.	3.4	62
165	Analysis of light scattering from surface roughness in hollow-core photonic bandgap fibers. Optics Express, 2012, 20, 20980.	3.4	61
166	100ÂkW peak power picosecond thulium-doped fiber amplifier system seeded by a gain-switched diode laser at 2Âμm. Optics Letters, 2013, 38, 1615.	3.3	60
167	Investigation of Brillouin effects in small-core holey optical fiber: lasing and scattering. Optics Letters, 2002, 27, 927.	3.3	59
168	A tunable WDM wavelength converter based on cross-phase modulation effects in normal dispersion holey fiber. IEEE Photonics Technology Letters, 2003, 15, 437-439.	2.5	59
169	Ultra-Broadband Bismuth-Doped Fiber Amplifier Covering a 115-nm Bandwidth in the O and E Bands. Journal of Lightwave Technology, 2021, 39, 795-800.	4.6	59
170	Highly efficient second-harmonic and sum-frequency generation of nanosecond pulses in a cascaded erbium-doped fiber:periodically poled lithium niobate source. Optics Letters, 1998, 23, 162.	3.3	58
171	Design of 7 and 19 cells core air-guiding photonic crystal fibers for low-loss, wide bandwidth and dispersion controlled operation. Optics Express, 2007, 15, 17577.	3.4	58
172	Archon: A Function Programmable Optical Interconnect Architecture for Transparent Intra and Inter Data Center SDM/TDM/WDM Networking. Journal of Lightwave Technology, 2015, 33, 1586-1595.	4.6	58
173	The Crystal Structure of the Extracellular 11-heme Cytochrome UndA Reveals a Conserved 10-heme Motif and Defined Binding Site for Soluble Iron Chelates. Structure, 2012, 20, 1275-1284.	3.3	56
174	Three mode Er^3+ ring-doped fiber amplifier for mode-division multiplexed transmission. Optics Express, 2013, 21, 10383.	3.4	56
175	Mo(V) Electron Paramagnetic Resonance Signals from the Periplasmic Nitrate Reductase of Thiosphaera Pantotropha. FEBS Journal, 1994, 226, 789-798.	0.2	55
176	Dual mode fused optical fiber couplers suitable for mode division multiplexed transmission. Optics Express, 2013, 21, 24326.	3.4	55
177	Frequency comb generation in a silicon ring resonator modulator. Optics Express, 2018, 26, 790.	3.4	55
178	The roles of CymA in support of the respiratory flexibility of <i>Shewanella oneidensis</i> MR-1. Biochemical Society Transactions, 2012, 40, 1217-1221.	3.4	54
179	32-core erbium/ytterbium-doped multicore fiber amplifier for next generation space-division multiplexed transmission system. Optics Express, 2017, 25, 32887.	3.4	54
180	Cytochrome <i>c</i> ₂ is essential for electron transfer to nitrous oxide reductase from physiological substrates in <i>Rhodobacter capsulatus</i> and can act as an electron donor to the reductase <i>in vitro</i> . FEBS Journal, 1991, 199, 677-683.	0.2	53

#	Article	IF	CITATIONS
181	Highly birefringent silica microfiber. Optics Letters, 2010, 35, 378.	3.3	53
182	Amplification of 12 OAM Modes in an air-core erbium doped fiber. Optics Express, 2015, 23, 28341.	3.4	53
183	Optical Orbital Angular Momentum Amplifier Based on an Air-Hole Erbium-Doped Fiber. Journal of Lightwave Technology, 2017, 35, 430-436.	4.6	53
184	The role of confinement loss in highly nonlinear silica holey fibers. IEEE Photonics Technology Letters, 2003, 15, 1246-1248.	2.5	52
185	Pulse compression at 106 \hat{l} /4m in dispersion-decreasing holey fibers. Optics Letters, 2006, 31, 3504.	3.3	52
186	All-solid highly nonlinear singlemode fibers with a tailored dispersion profile. Optics Express, 2011, 19, 66.	3.4	52
187	A photonic switch based on a gigantic, reversible optical nonlinearity of liquefying gallium. Applied Physics Letters, 1998, 73, 1787-1789.	3.3	51
188	Dispersion controlled highly nonlinear fibers for all-optical processing at telecoms wavelengths. Optical Fiber Technology, 2010, 16, 378-391.	2.7	51
189	Structural modeling of an outer membrane electron conduit from a metal-reducing bacterium suggests electron transfer via periplasmic redox partners. Journal of Biological Chemistry, 2018, 293, 8103-8112.	3.4	51
190	Fabrication of tubular anti-resonant hollow core fibers: modelling, draw dynamics and process optimization. Optics Express, 2019, 27, 20567.	3.4	51
191	Dissimilatory iron(III) reduction by Rhodobacter capsulatus. Microbiology (United Kingdom), 1996, 142, 765-774.	1.8	50
192	Holey optical fibres: Fundamental properties and device applications. Comptes Rendus Physique, 2003, 4, 175-186.	0.9	50
193	Resolving the contributions of the membrane-bound and periplasmic nitrate reductase systems to nitric oxide and nitrous oxide production in <i>Salmonella enterica</i> serovar Typhimurium. Biochemical Journal, 2012, 441, 755-762.	3.7	50
194	Transmission media for an SDM-based optical communication system. , 2015, 53, 44-51.		50
195	Mode Coupling Effects in Ring-Core Fibers for Space-Division Multiplexing Systems. Journal of Lightwave Technology, 2016, 34, 3365-3372.	4.6	50
196	Mitigation of Nonlinear Effects on WDM QAM Signals Enabled by Optical Phase Conjugation With Efficient Bandwidth Utilization. Journal of Lightwave Technology, 2017, 35, 971-978.	4.6	50
197	Passive Q-switching of fiber lasers using a broadband liquefying gallium mirror. Applied Physics Letters, 1999, 74, 3619-3621.	3.3	49
198	20 × 960-Gb/s Space-division-multiplexed 32QAM transmission over 60 km few-mode fiber. Optics Express, 2014, 22, 749.	3.4	49

#	Article	IF	CITATIONS
199	Characterization of Mode Coupling in Few-Mode FBG With Selective Mode Excitation. IEEE Photonics Technology Letters, 2015, 27, 1713-1716.	2.5	49
200	Broadband telecom to mid-infrared supercontinuum generation in a dispersion-engineered silicon germanium waveguide. Optics Letters, 2015, 40, 4118.	3.3	49
201	Long-Haul Dense Space-Division Multiplexed Transmission Over Low-Crosstalk Heterogeneous 32-Core Transmission Line Using a Partial Recirculating Loop System. Journal of Lightwave Technology, 2017, 35, 488-498.	4.6	49
202	How to make the propagation time through an optical fiber fully insensitive to temperature variations. Optica, 2017, 4, 659.	9.3	49
203	Photonic lantern broadband orbital angular momentum mode multiplexer. Optics Express, 2018, 26, 30042.	3.4	49
204	Wavelength-swept fiber laser with frequency shifted feedback and resonantly swept intra-cavity acoustooptic tunable filter. IEEE Journal of Selected Topics in Quantum Electronics, 1997, 3, 1087-1096.	2.9	48
205	Experimental demonstration of intermodal dispersion in a two-core optical fibre. Optics Communications, 1997, 143, 189-192.	2.1	48
206	Nonlinear switching in a 20-cm-long fiber Bragg grating. Optics Letters, 2000, 25, 536.	3.3	48
207	The NapF protein of the Escherichia coli periplasmic nitrate reductase system: demonstration of a cytoplasmic location and interaction with the catalytic subunit, NapA. Microbiology (United) Tj ETQq1 1 0.784.	314 1 g8T /C)ve rlø ck 10 Tf
208	Characterization of MtoD from Sideroxydans lithotrophicus: a cytochrome c electron shuttle used in lithoautotrophic growth. Frontiers in Microbiology, 2015, 6, 332.	3.5	48
209	Role of multiheme cytochromes involved in extracellular anaerobic respiration in bacteria. Protein Science, 2020, 29, 830-842.	7.6	48
210	A 36-channel x 10-GHz spectrally sliced pulse source based on supercontinuum generation in normally dispersive highly nonlinear holey fiber. IEEE Photonics Technology Letters, 2003, 15, 1689-1691.	2.5	47
211	Polarization-maintaining optical microfiber. Optics Letters, 2010, 35, 2034.	3.3	47
212	Homodyne OFDM with Optical Injection Locking for Carrier Recovery. Journal of Lightwave Technology, 2015, 33, 34-41.	4.6	47
213	Reconfigurable structured light generation in a multicore fibre amplifier. Nature Communications, 2020, 11, 3986.	12.8	47
214	Q-switched erbium doped fibre laser utilising a novel large mode area fibre. Electronics Letters, 1997, 33, 393.	1.0	46
215	Optical parametric oscillation in periodically poled lithium niobate driven by a diode-pumped Q-switched erbium fiber laser. Optics Letters, 1998, 23, 582.	3.3	46
216	An integrated biochemical system for nitrate assimilation and nitric oxide detoxification in <i>Bradyrhizobium japonicum</i> . Biochemical Journal, 2016, 473, 297-309.	3.7	46

#	Article	IF	CITATIONS
217	Nonlinear switching in fibre Bragg gratings. Optics Express, 1998, 3, 447.	3.4	45
218	Phase encoding and decoding of short pulses at 10 Gb/s using superstructured fiber Bragg gratings. IEEE Photonics Technology Letters, 2001, 13, 154-156.	2.5	45
219	UV generation in a pure-silica holey fiber. Applied Physics B: Lasers and Optics, 2003, 77, 291-298.	2.2	45
220	Compensation of Linear Distortions by Using XPM With Parabolic Pulses as a Time Lens. IEEE Photonics Technology Letters, 2008, 20, 1097-1099.	2.5	45
221	Optical properties of silicon germanium waveguides at telecommunication wavelengths. Optics Express, 2013, 21, 16690.	3.4	44
222	Minimizing differential modal gain in cladding-pumped EDFAs supporting four and six mode groups. Optics Express, 2014, 22, 21499.	3.4	44
223	High Power Diode-Seeded Fiber Amplifiers at 2 μm—From Architectures to Applications. IEEE Journal of Selected Topics in Quantum Electronics, 2014, 20, 525-536.	2.9	44
224	All-optical pulse reshaping and retiming systems incorporating pulse shaping fiber Bragg grating. Journal of Lightwave Technology, 2006, 24, 357-364.	4.6	43
225	Soluble Aldose Sugar Dehydrogenase from Escherichia coli. Journal of Biological Chemistry, 2006, 281, 30650-30659.	3.4	43
226	Towards efficient and broadband four-wave-mixing using short-length dispersion tailored lead silicate holey fibers. Optics Express, 2007, 15, 596.	3.4	43
227	Voltammetric characterization of the aerobic energy-dissipating nitrate reductase of <i>Paracoccus pantotrophus</i> : exploring the activity of a redox-balancing enzyme as a function of electrochemical potential. Biochemical Journal, 2008, 409, 159-168.	3.7	43
228	Fibre optical sensor for C2H2 gas using gas-filled photonic bandgap fibre reference cell. Sensors and Actuators B: Chemical, 2009, 139, 30-34.	7.8	43
229	Nonlinearity-Free Coherent Transmission in Hollow-Core Antiresonant Fiber. Journal of Lightwave Technology, 2019, 37, 909-916.	4.6	43
230	Adiabatically tapered splice for selective excitation of the fundamental mode in a multimode fiber. Optics Letters, 2009, 34, 2369.	3.3	42
231	Direct Selection and Amplification of Individual Narrowly Spaced Optical Comb Modes Via Injection Locking: Design and Characterization. Journal of Lightwave Technology, 2013, 31, 2287-2295.	4.6	42
232	Multi-Element Fiber Technology for Space-Division Multiplexing Applications. Optics Express, 2014, 22, 3787.	3.4	42
233	Dense WDM transmission at 2  μm enabled by an arrayed waveguide grating. Optics Letters, 2015, 40,	333 0 8.	42
234	Low loss and high performance interconnection between standard single-mode fiber and antiresonant hollow-core fiber. Scientific Reports, 2021, 11, 8799.	3.3	42

#	Article	IF	CITATIONS
235	Square Core Jacketed Air-Clad Fiber. Optics Express, 2006, 14, 10345.	3.4	41
236	Effects of soluble flavin on heterogeneous electron transfer between surface-exposed bacterial cytochromes and iron oxides. Geochimica Et Cosmochimica Acta, 2015, 163, 299-310.	3.9	41
237	Identification of two domains and distal histidine ligands to the four haems in the bacterial c-type cytochrome NapC; the prototype connector between quinol/quinone and periplasmic oxido-reductases. Biochemical Journal, 2002, 368, 425-432.	3.7	40
238	High-power, high-brightness, mJ Q-switched ytterbium-doped fibre laser. Electronics Letters, 2004, 40, 928.	1.0	40
239	Progress in Multichannel All-Optical Regeneration Based on Fiber Technology. IEEE Journal of Selected Topics in Quantum Electronics, 2012, 18, 689-700.	2.9	40
240	An Efficient Wavelength Converter Exploiting a Grating-Based Saw-Tooth Pulse Shaper. IEEE Photonics Technology Letters, 2008, 20, 1461-1463.	2.5	39
241	Quinol-cytochrome c Oxidoreductase and Cytochrome c4 Mediate Electron Transfer during Selenate Respiration in Thauera selenatis. Journal of Biological Chemistry, 2010, 285, 18433-18442.	3.4	38
242	Compact, high-pulse-energy, picosecond optical parametric oscillator. Optics Letters, 2010, 35, 3580.	3.3	38
243	High gain holmium-doped fibre amplifiers. Optics Express, 2016, 24, 13946.	3.4	38
244	106  W, picosecond Yb-doped fiber MOPA system with a radially polarized output beam. Optics Letters, 2018, 43, 4957.	3.3	38
245	A grating-based OCDMA coding-decoding system incorporating a nonlinear optical loop mirror for improved code recognition and noise reduction. Journal of Lightwave Technology, 2002, 20, 36-46.	4.6	37
246	First demonstration of all-optical QPSK signal regeneration in a novel multi-format phase sensitive amplifier. , 2010, , .		37
247	High-energy, in-band pumped erbium doped fiber amplifiers. Optics Express, 2012, 20, 18803.	3.4	37
248	200 W Diffraction limited, single-polarization, all-fiber picosecond MOPA. Optics Express, 2013, 21, 25883.	3.4	37
249	NapF Is a Cytoplasmic Iron-Sulfur Protein Required for Fe-S Cluster Assembly in the Periplasmic Nitrate Reductase. Journal of Biological Chemistry, 2004, 279, 49727-49735.	3.4	36
250	Compact high-power tunable three-level operation of double cladding Nd-doped fiber laser. IEEE Photonics Technology Letters, 2005, 17, 306-308.	2.5	36
251	Escherichia coli Cytochrome c Nitrite Reductase NrfA. Methods in Enzymology, 2008, 437, 63-77.	1.0	36
252	Remnant signal peptides on non-exported enzymes: implications for the evolution of prokaryotic respiratory chains. Microbiology (United Kingdom), 2009, 155, 3992-4004.	1.8	36

#	Article	IF	CITATIONS
253	Dispersion-shifted all-solid high index-contrast microstructured optical fiber for nonlinear applications at 155î¼m. Optics Express, 2009, 17, 20249.	3.4	36
254	Anti-resonant hexagram hollow core fibers. Optics Express, 2015, 23, 1289.	3.4	36
255	Amplification of femtosecond pulses in a passive, all-fiber soliton source. Optics Letters, 1992, 17, 1596.	3.3	35
256	Self-starting, passively mode-locked Fabry-Perot fiber soliton laser using nonlinear polarization evolution. IEEE Photonics Technology Letters, 1993, 5, 492-494.	2.5	35
257	Power scaling in passively mode-locked large-mode area fiber lasers. IEEE Photonics Technology Letters, 1998, 10, 1718-1720.	2.5	35
258	Highly Scalable Amplified Hybrid TDM/DWDM Array Architecture for Interferometric Fiber-Optic Sensor Systems. Journal of Lightwave Technology, 2013, 31, 882-888.	4.6	35
259	Nonlinear dynamic of picosecond pulse propagation in atmospheric air-filled hollow core fibers. Optics Express, 2018, 26, 8866.	3.4	35
260	High quality soliton loss-compensation in 38 km dispersion-decreasing fibre. Electronics Letters, 1995, 31, 1681-1682.	1.0	35
261	Ultra-short wavelength operation of thulium-doped fiber amplifiers and lasers. Optics Express, 2019, 27, 36699.	3.4	35
262	All-fiber sliding-frequency Er^3+/Yb^3+ soliton laser. Optics Letters, 1995, 20, 2381.	3.3	34
263	Experimental observation of nonlinear pulse compression in nonuniform Bragg gratings. Optics Letters, 1997, 22, 1837.	3.3	34
264	Noise properties and phase resolution of interferometer systems interrogated by narrowband fiber ASE sources. Journal of Lightwave Technology, 1999, 17, 2327-2335.	4.6	34
265	Diode or Tunnel-Diode Characteristics? Resolving the Catalytic Consequences of Proton Coupled Electron Transfer in a Multi-Centered Oxidoreductase. Journal of the American Chemical Society, 2005, 127, 14964-14965.	13.7	34
266	Polarization-Assisted Phase-Sensitive Processor. Journal of Lightwave Technology, 2015, 33, 1166-1174.	4.6	34
267	MicroStructure Element Method (MSEM): viscous flow model for the virtual draw of microstructured optical fibers. Optics Express, 2015, 23, 312.	3.4	34
268	Broad-band second-harmonic generation in holey optical fibers. IEEE Photonics Technology Letters, 2001, 13, 981-983.	2.5	33
269	Filtering Effects in a Spectrum-Sliced WDM System Using SOA-Based Noise Reduction. IEEE Photonics Technology Letters, 2004, 16, 680-682.	2.5	33
270	Reductive activation of nitrate reductases. Dalton Transactions, 2005, , 3580.	3.3	33

#	Article	IF	CITATIONS
271	Kinetic and thermodynamic resolution of the interactions between sulfite and the pentahaem cytochrome NrfA from <i>Escherichia coli</i> . Biochemical Journal, 2010, 431, 73-80.	3.7	33
272	Modeling Brillouin Gain Spectrum of Solid and Microstructured Optical Fibers Using a Finite Element Method. Journal of Lightwave Technology, 2011, 29, 22-30.	4.6	33
273	Large aperture PPMgLN based high-power optical parametric oscillator at 38 µm pumped by a nanosecond linearly polarized fiber MOPA. Optics Express, 2012, 20, 15008.	3.4	33
274	Using direct electrochemistry to probe rate limiting events during nitrate reductase turnover. Faraday Discussions, 2000, 116, 155-169.	3.2	32
275	Extruded single-mode high-index-core one-dimensional microstructured optical fiber with high index-contrast for highly nonlinear optical devices. Applied Physics Letters, 2005, 87, 081110.	3.3	32
276	High-power, high repetition-rate, green-pumped, picosecond LBO optical parametric oscillator. Optics Express, 2012, 20, 7008.	3.4	32
277	41.6 Tbit/s C-Band SDM OFDM Transmission Through 12 Spatial and Polarization Modes Over 74.17 km Few Mode Fiber. Journal of Lightwave Technology, 2015, 33, 1440-1444.	4.6	32
278	Reconfigurable multilevel phase-shift keying encoder-decoder for all-optical networks. IEEE Photonics Technology Letters, 2003, 15, 431-433.	2.5	31
279	Efficient white light generation in secondary cores of holey fibers. Optics Express, 2007, 15, 3729.	3.4	31
280	Slowing of Pulses to c/10 With Subwatt Power Levels and Low Latency Using Brillouin Amplification in a Bismuth-Oxide Optical Fiber. Journal of Lightwave Technology, 2007, 25, 216-221.	4.6	31
281	Features of a twinâ€arginine signal peptide required for recognition by a Tat proofreading chaperone. FEBS Letters, 2008, 582, 3979-3984.	2.8	31
282	Analysis of a two-channel 2R all-optical regenerator based on a counter-propagating configuration. Optics Express, 2008, 16, 2264.	3.4	31
283	The nitric oxide response in plant-associated endosymbiotic bacteria. Biochemical Society Transactions, 2011, 39, 1880-1885.	3.4	31
284	Optimizing the pumping configuration for the power scaling of in-band pumped erbium doped fiber amplifiers. Optics Express, 2012, 20, 13886.	3.4	31
285	Modulator-free quadrature amplitude modulation signal synthesis. Nature Communications, 2014, 5, 5911.	12.8	31
286	High-power chirped-pulse all-fiber amplification system based on large-mode-area fiber gratings. Optics Letters, 1999, 24, 566.	3.3	30
287	Mo(V) co-ordination in the periplasmic nitrate reductase from Paracoccus pantotrophus probed by electron nuclear double resonance (ENDOR) spectroscopy. Biochemical Journal, 2002, 363, 817-823.	3.7	30
288	Synchronously pumped optical parametric oscillator driven by a femtosecond mode-locked fiber laser. Optics Letters, 2002, 27, 1052.	3.3	30

#	Article	IF	CITATIONS
289	Guided-wave second-harmonic generation in a LiNbO_3 nonlinear photonic crystal. Optics Letters, 2006, 31, 1232.	3.3	30
290	Optical Fiber Fabrication Using Novel Gas-Phase Deposition Technique. Journal of Lightwave Technology, 2011, 29, 912-915.	4.6	30
291	40 Gb/s WDM Transmission Over 1.15-km HC-PBGF Using an InP-Based Mach-Zehnder Modulator at 2 μm. Journal of Lightwave Technology, 2016, 34, 1706-1711.	4.6	30
292	The <scp><i>P</i></scp> <i>aracoccus denitrificans</i> <scp>N</scp> ar <scp>K</scp> â€like nitrate and nitrite transporters—probing nitrate uptake and nitrate/nitrite exchange mechanisms. Molecular Microbiology, 2017, 103, 117-133.	2.5	30
293	All-optical mode-group multiplexed transmission over a graded-index ring-core fiber with single radial mode. Optics Express, 2017, 25, 13773.	3.4	30
294	High-average-power picosecond mid-infrared OP-GaAs OPO. Optics Express, 2020, 28, 5741.	3.4	30
295	Ytterbium-doped large-core fibre laser with 272â€W output power. Electronics Letters, 2003, 39, 977.	1.0	29
296	Near-zero dispersion, highly nonlinear lead-silicate W-type fiber for applications at 155μm. Optics Express, 2010, 18, 15747.	3.4	29
297	X-ray tomography for structural analysis of microstructured and multimaterial optical fibers and preforms. Optics Express, 2014, 22, 26181.	3.4	29
298	WDM Transmission With In-Line Amplification at 1.3 <i>μ</i> m Using a Bi-Doped Fiber Amplifier. Journal of Lightwave Technology, 2019, 37, 1826-1830.	4.6	29
299	Resolving Complexity in the Interactions of Redox Enzymes and Their Inhibitors:Â Contrasting Mechanisms for the Inhibition of a CytochromecNitrite Reductase Revealed by Protein Film Voltammetryâ€. Biochemistry, 2004, 43, 15086-15094.	2.5	28
300	Gridless optical networking field trial: flexible spectrum switching, defragmentation and transport of 10G/40G/100G/555G over 620-km field fiber. Optics Express, 2011, 19, B277.	3.4	28
301	The production and detoxification of a potent cytotoxin, nitric oxide, by pathogenic enteric bacteria. Biochemical Society Transactions, 2011, 39, 1876-1879.	3.4	28
302	Resolution of Key Roles for the Distal Pocket Histidine in Cytochrome <i>c</i> Nitrite Reductases. Journal of the American Chemical Society, 2015, 137, 3059-3068.	13.7	28
303	Diode-pumped, high-energy, single transverse mode Q-switch fibre laser. Electronics Letters, 1997, 33, 1955.	1.0	27
304	Soliton Spectral Tunneling in Dispersion-Controlled Holey Fibers. IEEE Photonics Technology Letters, 2008, 20, 1414-1416.	2.5	27
305	High fidelity femtosecond pulses from an ultrafast fiber laser system via adaptive amplitude and phase pre-shaping. Optics Express, 2008, 16, 15074.	3.4	27
306	Optical Propulsion of Individual and Clustered Microspheres along Sub-Micron Optical Wires. Japanese Journal of Applied Physics, 2008, 47, 6716-6718.	1.5	27

#	ARTICLE	IF	CITATIONS
307	The relationship between redox enzyme activity and electrochemical potential—cellular and mechanistic implications from protein film electrochemistry. Physical Chemistry Chemical Physics, 2011, 13, 7720.	2.8	27
308	Fiber-laser-pumped, high-energy, mid-IR, picosecond optical parametric oscillator with a high-harmonic cavity. Optics Letters, 2015, 40, 3288.	3.3	27
309	Roadmap on multimode photonics. Journal of Optics (United Kingdom), 2022, 24, 083001.	2.2	27
310	Demonstration of a 64-chip OCDMA system using superstructured fiber gratings and time-gating detection. IEEE Photonics Technology Letters, 2001, 13, 1239-1241.	2.5	26
311	Redox-triggered events in cytochrome c nitrite reductase. Bioelectrochemistry, 2004, 63, 43-47.	4.6	26
312	Investigation of the redox centres of periplasmic selenate reductase from <i>Thauera selenatis</i> by EPR spectroscopy. Biochemical Journal, 2007, 408, 19-28.	3.7	26
313	PPMgLN-Based High-Power Optical Parametric Oscillator Pumped by Yb \$^{{m 3}{m +}}\$-Doped Fiber Amplifier Incorporates Active Pulse Shaping. IEEE Journal of Selected Topics in Quantum Electronics, 2009, 15, 385-392.	2.9	26
314	High-power, variable repetition rate, picosecond optical parametric oscillator pumped by an amplified gain-switched diode. Optics Express, 2010, 18, 7602.	3.4	26
315	Field demonstration of mode-division multiplexing upgrade scenarios on commercial networks. Optics Express, 2013, 21, 31036.	3.4	26
316	Impact of structural distortions on the performance of hollow-core photonic bandgap fibers. Optics Express, 2014, 22, 2735.	3.4	26
317	Optical injection locking-based amplification in phase-coherent transfer of optical frequencies. Optics Letters, 2015, 40, 4198.	3.3	26
318	High-energy, near- and mid-IR picosecond pulses generated by a fiber-MOPA-pumped optical parametric generator and amplifier. Optics Express, 2015, 23, 12613.	3.4	26
319	Lotus-Shaped Negative Curvature Hollow Core Fiber With 10.5 dB/km at 1550 nm Wavelength. Journal of Lightwave Technology, 2018, 36, 1213-1219.	4.6	26
320	Parametric oscillator directly pumped by a 155-µm erbium-fiber laser. Optics Letters, 1999, 24, 975.	3.3	25
321	All-optical modulation and demultiplexing systems with significant timing jitter tolerance through incorporation of pulse-shaping fiber Bragg gratings. IEEE Photonics Technology Letters, 2002, 14, 203-205.	2.5	25
322	2R regenerator based on a 2-m-long highly nonlinear bismuth oxide fiber. Optics Express, 2006, 14, 5038.	3.4	25
323	Nonlinear tapered holey fibers with high stimulated Brillouin scattering threshold and controlled dispersion. Journal of the Optical Society of America B: Optical Physics, 2007, 24, 2185.	2.1	25

Respiration of Nitrate and Nitrite. EcoSal Plus, 2008, 3, .

5.4 25

#	Article	IF	CITATIONS
325	Analysis of structural MtrC models based on homology with the crystal structure of MtrF. Biochemical Society Transactions, 2012, 40, 1181-1185.	3.4	25
326	Compact Optical Comb Generator Using InP Tunable Laser and Push-Pull Modulator. IEEE Photonics Technology Letters, 2015, 27, 217-220.	2.5	25
327	Transmission of 61 C-Band Channels Over Record Distance of Hollow-Core-Fiber With L-Band Interferers. Journal of Lightwave Technology, 2021, 39, 813-820.	4.6	25
328	Low-loss all-fiber acousto-optic tunable filter. Optics Letters, 1997, 22, 96.	3.3	24
329	Investigation of Four-Wavelength Regenerator Using Polarization- and Direction-Multiplexing. IEEE Photonics Technology Letters, 2008, 20, 1676-1678.	2.5	24
330	Exploring the biochemistry at the extracellular redox frontier of bacterial mineral Fe(III) respiration. Biochemical Society Transactions, 2012, 40, 493-500.	3.4	24
331	Accurate modelling of fabricated hollow-core photonic bandgap fibers. Optics Express, 2015, 23, 23117.	3.4	24
332	Intermodal Four-Wave Mixing and Parametric Amplification in Kilometer-Long Multimode Fibers. Journal of Lightwave Technology, 2017, 35, 5296-5305.	4.6	24
333	295-kW peak power picosecond pulses from a thulium-doped-fiber MOPA and the generation of watt-level >25-octave supercontinuum extending up to 5 î¼m. Optics Express, 2018, 26, 6490.	3.4	24
334	NosL is a dedicated copper chaperone for assembly of the Cu _Z center of nitrous oxide reductase. Chemical Science, 2019, 10, 4985-4993.	7.4	24
335	High Spatial Density 6-Mode 7-Core Fiber Amplifier for L-Band Operation. Journal of Lightwave Technology, 2020, 38, 2938-2943.	4.6	24
336	Wavelength-tunable high-power picosecond pulses from a fiber-pumped diode-seeded high-gain parametric amplifier. Optics Letters, 1998, 23, 1588.	3.3	23
337	All-Optical Packet Compression Based on Time-to-Wavelength Conversion. IEEE Photonics Technology Letters, 2004, 16, 1688-1690.	2.5	23
338	High energy femtosecond fiber chirped pulse amplification system with adaptive phase control. Optics Express, 2008, 16, 5813.	3.4	23
339	The <i>c</i> -Type Cytochrome OmcA Localizes to the Outer Membrane upon Heterologous Expression in <i>Escherichia coli</i> . Journal of Bacteriology, 2008, 190, 5127-5131.	2.2	23
340	Efficient All-Optical Wavelength-Conversion Scheme Based on a Saw-Tooth Pulse Shaper. IEEE Photonics Technology Letters, 2009, 21, 1837-1839.	2.5	23
341	Compact, high-pulse-energy, high-power, picosecond master oscillator power amplifier. Optics Express, 2014, 22, 21938.	3.4	23
342	Optical Fourier synthesis of high-repetition-rate pulses. Optica, 2015, 2, 18.	9.3	23

#	Article	IF	CITATIONS
343	Experimental Demonstration of Dual O+C-Band WDM Transmission Over 50-km SSMF With Direct Detection. Journal of Lightwave Technology, 2020, 38, 2278-2284.	4.6	23
344	Extruded tellurite antiresonant hollow core fiber for Mid-IR operation. Optics Express, 2020, 28, 16542.	3.4	23
345	Reduction of interchannel interference noise in a two-channel grating-based OCDMA system using a nonlinear optical loop mirror. IEEE Photonics Technology Letters, 2001, 13, 529-531.	2.5	22
346	High gain efficiency amplifier based on an erbium doped aluminosilicate holey fiber. Optics Express, 2004, 12, 3452.	3.4	22
347	Optimisation of cascaded Yb fiber amplifier chains using numerical-modelling. Optics Express, 2006, 14, 12846.	3.4	22
348	Designing Tapered Holey Fibers for Soliton Compression. IEEE Journal of Quantum Electronics, 2008, 44, 192-198.	1.9	22
349	Green-pumped, picosecond MgO:PPLN optical parametric oscillator. Journal of the Optical Society of America B: Optical Physics, 2012, 29, 144.	2.1	22
350	Nonlinear Generation of Ultra-Flat Broadened Spectrum Based on Adaptive Pulse Shaping. Journal of Lightwave Technology, 2012, 30, 1971-1977.	4.6	22
351	Erbium-doped multi-element fiber amplifiers for space-division multiplexing operations. Optics Letters, 2013, 38, 582.	3.3	22
352	High-energy diode-seeded nanosecond 2  μm fiber MOPA systems incorporating active pulse shaping. Optics Letters, 2014, 39, 1569.	3.3	22
353	Comparative structure-potentio-spectroscopy of the Shewanella outer membrane multiheme cytochromes. Current Opinion in Electrochemistry, 2017, 4, 199-205.	4.8	22
354	Hollow Core NANFs with Five Nested Tubes and Record Low Loss at 850, 1060, 1300 and 1625nm. , 2021, , .		22
355	Comparison between nonlinear and linear spectrographic techniques for the complete characterization of high bit-rate pulses used in optical communications. IEEE Photonics Technology Letters, 2005, 17, 1914-1916.	2.5	21
356	Hollow-core photonic bandgap fibers based on a square lattice cladding. Optics Letters, 2007, 32, 2282.	3.3	21
357	Feasibility Study of SOA-Based Noise Suppression for Spectral Amplitude Coded OCDMA. Journal of Lightwave Technology, 2007, 25, 394-401.	4.6	21
358	Time domain add–drop multiplexing scheme enhanced using a saw-tooth pulse shaper. Optics Express, 2009, 17, 8362.	3.4	21
359	Wavelength Conversion in a Short Length of a Solid Lead–Silicate Fiber. IEEE Photonics Technology Letters, 2010, 22, 628-630.	2.5	21
360	Design of Four-Mode Erbium Doped Fiber Amplifier with Low Differential Modal Gain for Modal Division Multiplexed Transmissions. , 2013, , .		21

#	Article	IF	CITATIONS
361	Ultra-low NA step-index large mode area Yb-doped fiber with a germanium doped cladding for high power pulse amplification. Optics Letters, 2020, 45, 3828.	3.3	21
362	Experimental investigation of picosecond pulse reflection from fiber gratings. Optics Letters, 1995, 20, 282.	3.3	20
363	OTDM to WDM format conversion based on quadratic cascading in a periodically poled lithium niobate waveguide. Optics Express, 2010, 18, 10282.	3.4	20
364	1.06 \$mu\$m Picosecond Pulsed, Normal Dispersion Pumping for Generating Efficient Broadband Infrared Supercontinuum in Meter-Length Single-Mode Tellurite Holey Fiber With High Raman Gain Coefficient. Journal of Lightwave Technology, 2011, 29, 3461-3469.	4.6	20
365	Development of a proteoliposome model to probe transmembrane electron-transfer reactions. Biochemical Society Transactions, 2012, 40, 1257-1260.	3.4	20
366	Phase Sensitivity Characterization in Fiber-Optic Sensor Systems Using Amplifiers and TDM. Journal of Lightwave Technology, 2013, 31, 1645-1653.	4.6	20
367	Controlling electron transfer at the microbe–mineral interface. Proceedings of the National Academy of Sciences of the United States of America, 2013, 110, 7537-7538.	7.1	20
368	Optical Phase Quantizer Based on Phase Sensitive Four Wave Mixing at Low Nonlinear Phase Shifts. IEEE Photonics Technology Letters, 2014, 26, 2146-2149.	2.5	20
369	Broadband silica-based thulium doped fiber amplifier employing multi-wavelength pumping. Optics Express, 2016, 24, 23001.	3.4	20
370	Bandwidth enhancement of inter-modal four wave mixing Bragg scattering by means of dispersion engineering. APL Photonics, 2019, 4, 022902.	5.7	20
371	Ultrafast laser-scanning optical resolution photoacoustic microscopy at up to 2 million A-lines per second. Journal of Biomedical Optics, 2018, 23, 1.	2.6	20
372	Compact micro-optic based components for hollow core fibers. Optics Express, 2020, 28, 1518.	3.4	20
373	QPSK Phase and Amplitude Regeneration at 56 Gbaud in a Novel Idler-Free Non-Degenerate Phase Sensitive Amplifier. , 2011, , .		20
374	A silica based highly nonlinear fibre with improved threshold for stimulated brillouin scattering. , 2010, , .		19
375	Analysis of multiple haloarchaeal genomes suggests that the quinoneâ€dependent respiratory nitric oxide reductase is an important source of nitrous oxide in hypersaline environments. Environmental Microbiology Reports, 2017, 9, 788-796.	2.4	19
376	Intermodal Bragg-Scattering Four Wave Mixing in Silicon Waveguides. Journal of Lightwave Technology, 2019, 37, 1680-1685.	4.6	19
377	A dual functional redox enzyme maturation protein for respiratory and assimilatory nitrate reductases in bacteria. Molecular Microbiology, 2019, 111, 1592-1603.	2.5	19
378	Long-Length and Thermally Stable High-Finesse Fabry-Perot Interferometers Made of Hollow Core Optical Fiber. Journal of Lightwave Technology, 2020, 38, 2423-2427.	4.6	19

#	Article	IF	CITATIONS
379	Highly efficient ÂTm ³⁺ doped germanate large mode area single mode fiber laser. Optical Materials Express, 2019, 9, 4115.	3.0	19
380	Periodically amplified system based on loss compensating dispersion decreasing fibre. Electronics Letters, 1996, 32, 373.	1.0	18
381	The role of multihaem cytochromes in the respiration of nitrite in <i>Escherichia coli</i> and Fe(III) in <i>Shewanella oneidensis</i> . Biochemical Society Transactions, 2008, 36, 1005-1010.	3.4	18
382	Embedded Optical Microfiber Coil Resonator With Enhanced High-\$Q\$. IEEE Photonics Technology Letters, 2010, , .	2.5	18
383	Control of Material Transport Through Pulse Shape Manipulation—A Development Toward Designer Pulses. IEEE Journal of Selected Topics in Quantum Electronics, 2014, 20, 51-63.	2.9	18
384	Optical chopper-based re-circulating loop for few-mode fiber transmission. Optics Letters, 2014, 39, 1181.	3.3	18
385	Efficient high-harmonic generation from a stable and compact ultrafast Yb-fiber laser producing 100ÂμJ, 350Âfs pulses based on bendable photonic crystal fiber. Applied Physics B: Lasers and Optics, 2017, 123, 43.	2.2	18
386	Super-broadband on-chip continuous spectral translation unlocking coherent optical communications beyond conventional telecom bands. Nature Communications, 2022, 13, .	12.8	18
387	Fiber-DFB laser array pumped with a single 1-W CW Yb-fiber laser. IEEE Photonics Technology Letters, 2003, 15, 655-657.	2.5	17
388	Wavelength and Duration-Tunable 10-GHz 1.3-ps Pulse Source Using Dispersion Decreasing Fiber-Based Distributed Raman Amplification. IEEE Photonics Technology Letters, 2004, 16, 1167-1169.	2.5	17
389	Synchronously pumped optical parametric oscillator with a repetition rate of 81.8 GHz. IEEE Photonics Technology Letters, 2005, 17, 483-485.	2.5	17
390	Brillouin characterization of holey optical fibers. Optics Letters, 2006, 31, 2541.	3.3	17
391	Brillouin assisted slow-light enhancement via Fabry-Perot cavity effects. Optics Express, 2007, 15, 5126.	3.4	17
392	Four-Channel All-Fiber Dispersion-Managed 2R Regenerator. IEEE Photonics Technology Letters, 2008, 20, 1169-1171.	2.5	17
393	56-W Frequency-Doubled Source at 530 nm Pumped by a Single-Mode, Single-Polarization, Picosecond, Yb\$^{3+}\$-Doped Fiber MOPA. IEEE Photonics Technology Letters, 2010, 22, 893-895.	2.5	17
394	Excitation of individual Raman Stokes lines in the visible regime using rectangular-shaped nanosecond optical pulses at 530 nm. Optics Letters, 2010, 35, 2433.	3.3	17
395	Field-Trial of an All-Optical PSK Regenerator/Multicaster in a 40 Gbit/s, 38 Channel DWDM Transmission Experiment. Journal of Lightwave Technology, 2012, 30, 512-520.	4.6	17
396	Leakage channel fibers with microstuctured cladding elements: A unique LMA platform. Optics Express, 2014, 22, 8574.	3.4	17

#	Article	IF	CITATIONS
397	Modal content in hypocycloid Kagomé hollow core photonic crystal fibers. Optics Express, 2016, 24, 15798.	3.4	17
398	All-optical Phase Regeneration with Record PSA Extinction Ratio in a Low-birefringence Silicon Germanium Waveguide. Journal of Lightwave Technology, 2016, 34, 3993-3998.	4.6	17
399	Multi-Band Direct-Detection Transmission Over an Ultrawide Bandwidth Hollow-Core NANF. Journal of Lightwave Technology, 2020, 38, 2849-2857.	4.6	17
400	Fiber Design For High-Power Low-Cost Yb:Al-Doped Fiber Laser Operating at 980 nm. IEEE Journal of Selected Topics in Quantum Electronics, 2007, 13, 588-597.	2.9	16
401	Design of a Bragg fiber with large mode area for mid-infrared applications. Optics Express, 2011, 19, 21295.	3.4	16
402	Optical racetrack ring-resonator based on two U-bent microfibers. Applied Physics Letters, 2011, 98, 021109.	3.3	16
403	Gamma irradiation of minimal latency Hollow-Core Photonic Bandgap Fibres. Journal of Instrumentation, 2013, 8, C12010-C12010.	1.2	16
404	Polarization-Insensitive Four-Wave-Mixing-Based Wavelength Conversion in Few-Mode Optical Fibers. Journal of Lightwave Technology, 2018, 36, 3678-3683.	4.6	16
405	Fully integrated optical isolators for space division multiplexed (SDM) transmission. APL Photonics, 2019, 4, .	5.7	16
406	Experimental characterization of an o-band bismuth-doped fiber amplifier. Optics Express, 2021, 29, 15345.	3.4	16
407	The generation of femtosecond optical vortex beams with megawatt powers directly from a fiber based Mamyshev oscillator. Nanophotonics, 2022, 11, 847-854.	6.0	16
408	977-nm All-Fiber DFB Laser. IEEE Photonics Technology Letters, 2004, 16, 2442-2444.	2.5	15
409	40 GHz adiabatic compression of a modulator based dual frequency beat signal using Raman amplification in dispersion decreasing fiber. Optics Express, 2004, 12, 2187.	3.4	15
410	OTDM add-drop multiplexer based on time-frequency signal processing. Journal of Lightwave Technology, 2006, 24, 2720-2732.	4.6	15
411	Stable and Efficient Generation of High Repetition Rate (\$>\$160 GHz) Subpicosecond Optical Pulses. IEEE Photonics Technology Letters, 2011, 23, 540-542.	2.5	15
412	Processing of optical combs with fiber optic parametric amplifiers. Optics Express, 2012, 20, 10059.	3.4	15
413	Broadband, Flat Frequency Comb Generated Using Pulse Shaping-Assisted Nonlinear Spectral Broadening. IEEE Photonics Technology Letters, 2013, 25, 543-545.	2.5	15
414	Fast and broadband fiber dispersion measurement with dense wavelength sampling. Optics Express, 2014, 22, 943.	3.4	15

#	Article	IF	CITATIONS
415	Laser frequency stabilization and spectroscopy at 2051 nm using a compact CO ₂ -filled Kagome hollow core fiber gas-cell system. Optics Express, 2018, 26, 28621.	3.4	15
416	Picosecond all-optical switching and dark pulse generation in a fibre-optic network using a plasmonic metamaterial absorber. Applied Physics Letters, 2018, 113, .	3.3	15
417	The Thermal Phase Sensitivity of Both Coated and Uncoated Standard and Hollow Core Fibers Down to Cryogenic Temperatures. Journal of Lightwave Technology, 2020, 38, 2477-2484.	4.6	15
418	Compact, high repetition rate, 42 MW peak power, 1925 nm, thulium-doped fiber chirped-pulse amplification system with dissipative soliton seed laser. Optics Express, 2019, 27, 36741.	3.4	15
419	Beam-Steering All-Optical Switch for Multi-Core Fibers. , 2017, , .		15
420	Rapidly reconfigurable optical phase encoder-decoders based on fiber Bragg gratings. IEEE Photonics Technology Letters, 2006, 18, 1216-1218.	2.5	14
421	Full Characterization of Low-Power Picosecond Pulses From a Gain-Switched Diode Laser Using Electrooptic Modulation-Based Linear FROG. IEEE Photonics Technology Letters, 2008, 20, 505-507.	2.5	14
422	Comparative study of the effective single mode operational bandwidth in sub-wavelength optical wires and conventional single-mode fibers. Optics Express, 2009, 17, 16619.	3.4	14
423	Field Experiments With a Grooming Switch for OTDM Meshed Networking. Journal of Lightwave Technology, 2010, 28, 316-327.	4.6	14
424	The Multipeak Phenomena and Nonlinear Effects in \${Q}\$-Switched Fiber Lasers. IEEE Photonics Technology Letters, 2011, 23, 1763-1765.	2.5	14
425	Real-time prediction of structural and optical properties of hollow-core photonic bandgap fibers during fabrication. Optics Letters, 2013, 38, 1382.	3.3	14
426	All-optical phase regeneration of 40Gbit/s DPSK signals in a black-box phase sensitive amplifier. , 2010, ,		14
427	The influence of chelating agents upon the dissimilatory reduction of Fe(III) byShewanella putrefaciens. Part 2. Oxo-and hydroxo-bridged polynuclear Fe(III) complexes. BioMetals, 1996, 9, 291-301.	4.1	13
428	Wavelength tunable 10-GHz 3-ps pulse source using a dispersion decreasing fiber-based nonlinear optical loop mirror. IEEE Journal of Selected Topics in Quantum Electronics, 2004, 10, 181-185.	2.9	13
429	Wide Bandwidth Experimental Study of Nondegenerate Phase-Sensitive Amplifiers in Single- and Dual-Pump Configurations. IEEE Photonics Technology Letters, 2010, 22, 1781-1783.	2.5	13
430	Modulation format conversion employing coherent optical superposition. Optics Express, 2012, 20, B322.	3.4	13
431	Electron Transport at the Microbe–Mineral Interface: a synthesis of current research challenges. Biochemical Society Transactions, 2012, 40, 1163-1166.	3.4	13
432	Yb-fiber amplifier pumped idler-resonant PPLN optical parametric oscillator producing 90 femtosecond pulses with high beam quality. Applied Physics B: Lasers and Optics, 2014, 117, 987-993.	2.2	13

#	Article	IF	CITATIONS
433	Multicore and multimode optical amplifiers for space division multiplexing. , 2020, , 301-333.		13
434	High Gain, Low Noise, Spectral-Gain-Controlled, Broadband Lumped Fiber Raman Amplifier. Journal of Lightwave Technology, 2021, 39, 1458-1463.	4.6	13
435	40 GHz soliton train generation through multisoliton pulse propagation in a dispersion varying optical fiber circuit. IEEE Photonics Technology Letters, 1994, 6, 1380-1382.	2.5	12
436	Spectral features associated with nonlinear pulse compression in Bragg gratings. Optics Letters, 2000, 25, 740.	3.3	12
437	Seeded erbiumâ^•ytterbium codoped fibre amplifier source with 87â€W of single-frequency output power. Electronics Letters, 2003, 39, 1717.	1.0	12
438	Non-silica microstructured optical fibers for mid-IR supercontinuum generation from 2 l̂¼m - 5 l̂¼m. , 2006, , .		12
439	Microstructured fibers for broadband wavefront filtering in the mid-IR. Optics Express, 2006, 14, 11773.	3.4	12
440	Development of a viologen-based microtiter plate assay for the analysis of oxyanion reductase activity: Application to the membrane-bound selenate reductase from Enterobacter cloacae SLD1a-1. Analytical Biochemistry, 2006, 358, 289-294.	2.4	12
441	Optical grooming switch with regenerative functionality for transparent interconnection of networks. Optics Express, 2009, 17, 15173.	3.4	12
442	All-Optical 160-Gbit/s Retiming System Using Fiber Grating Based Pulse Shaping Technology. Journal of Lightwave Technology, 2009, 27, 1135-1141.	4.6	12
443	Feed-forward true carrier extraction of high baud rate phase shift keyed signals using photonic modulation stripping and low-bandwidth electronics. Optics Express, 2011, 19, 26594.	3.4	12
444	Selective amplification of frequency comb modes via optical injection locking of a semiconductor laser: influence of adjacent unlocked comb modes. Proceedings of SPIE, 2013, , .	0.8	12
445	Gain equalization of a six-mode-group ring core multimode EDFA. , 2014, , .		12
446	Low Thermal Sensitivity Hollow Core Fiber for Optically-Switched Data Centers. Journal of Lightwave Technology, 2020, 38, 2703-2709.	4.6	12
447	High-power, electronically controlled source of user-defined vortex and vector light beams based on a few-mode fiber amplifier. Photonics Research, 2021, 9, 856.	7.0	12
448	Numerical and experimental study on the impact of chromatic dispersion on O-band direct-detection transmission. Applied Optics, 2021, 60, 4383.	1.8	12
449	Thinly coated hollow core fiber for improved thermal phase-stability performance. Optics Letters, 2021, 46, 5177.	3.3	12

450 InP-based Optical Comb-locked Tunable Transmitter. , 2016, , .

#	Article	IF	CITATIONS
451	High-power, high-efficiency, all-fiberized-laser-pumped, 260-nm, deep-UV laser for bacterial deactivation. Optics Express, 2021, 29, 42485.	3.4	12
452	Passive Q-switching of an Er3+:Yb3+ fibre laser with a fibrised liquefying gallium mirror. Optics Communications, 1999, 166, 239-243.	2.1	11
453	Cross-wavelength all-optical switching using nonlinearity of liquefying gallium. Optics Express, 1999, 5, 157.	3.4	11
454	Cross-phase modulation effects in nonlinear fiber Bragg gratings. Journal of the Optical Society of America B: Optical Physics, 2000, 17, 345.	2.1	11
455	Optical parametric oscillator with a pulse repetition rate of 39 GHz and 21-W signal average output power in the spectral region near 15 µm. Optics Letters, 2005, 30, 290.	3.3	11
456	A 16-Channel Reconfigurable OCDMA/DWDM System Using Continuous Phase-Shift SSFBGs. IEEE Journal of Selected Topics in Quantum Electronics, 2007, 13, 1480-1486.	2.9	11
457	Timing Jitter Tolerant All-Optical TDM Demultiplexing Using a Saw-Tooth Pulse Shaper. IEEE Photonics Technology Letters, 2008, 20, 1992-1994.	2.5	11
458	Dispersion Management in Highly Nonlinear, Carbon Disulfide Filled Holey Fibers. IEEE Photonics Technology Letters, 2008, 20, 1449-1451.	2.5	11
459	All-Optical Signal Processing of Periodic Signals Using a Brillouin Gain Comb. Journal of Lightwave Technology, 2008, 26, 3110-3117.	4.6	11
460	Beating the electronics bottleneck. Nature Photonics, 2009, 3, 562-564.	31.4	11
461	Retiming of Short Pulses Using Quadratic Cascading in a Periodically Poled Lithium Niobate Waveguide. IEEE Photonics Technology Letters, 2011, 23, 94-96.	2.5	11
462	Temporally and spatially shaped fully-fiberized ytterbium-doped pulsed MOPA. Laser Physics Letters, 2011, 8, 747-753.	1.4	11
463	Brillouin Suppressed Highly Nonlinear Fibers. , 2012, , .		11
464	Few-mode multi-element fiber amplifier for mode division multiplexing. Optics Express, 2014, 22, 29031.	3.4	11
465	Picometer-scale surface roughness measurements inside hollow glass fibres. Optics Express, 2014, 22, 29554.	3.4	11
466	100-GHz Grid-Aligned Multi-Channel Polarization Insensitive Black-Box Wavelength Converter. Journal of Lightwave Technology, 2014, 32, 3027-3035.	4.6	11
467	A quasi-mode interpretation of radiation modes in long-period fiber gratings. IEEE Journal of Quantum Electronics, 2003, 39, 1135-1142.	1.9	10
468	The Prokaryotic Nitrate Reductases. , 2007, , 21-35.		10

#	Article	IF	CITATIONS
469	The effect of periodicity on the defect modes of large mode area microstructured fibers. Optics Express, 2008, 16, 18631.	3.4	10
470	Vector Mode effects in Few Moded Erbium Doped Fiber Amplifiers. , 2013, , .		10
471	Anisotropic Superattenuation of Capillary Waves on Driven Glass Interfaces. Physical Review Letters, 2017, 119, 235501.	7.8	10
472	Optical Fiber Delay Lines in Microwave Photonics: Sensitivity to Temperature and Means to Reduce it. Journal of Lightwave Technology, 2021, 39, 2311-2318.	4.6	10
473	Selective wavelength conversion in a few-mode fiber. Optics Express, 2019, 27, 24072.	3.4	10
474	Transmission of 6 ps linear pulses over 50 km of standard fiber using midpoint spectral inversion to eliminate dispersion. IEEE Journal of Quantum Electronics, 1994, 30, 2114-2119.	1.9	9
475	All-optical modulation of 40 GHz beat frequency conversion soliton source. Electronics Letters, 1995, 31, 1362-1364.	1.0	9
476	Investigation of fiber grating-based performance limits in pulse stretching and recompression schemes using bidirectional reflection from a linearly chirped fiber grating. IEEE Photonics Technology Letters, 1995, 7, 1436-1438.	2.5	9
477	Direct characterization of the spatial effective refractive index profile in Bragg gratings. IEEE Photonics Technology Letters, 2005, 17, 2685-2687.	2.5	9
478	Silica-based highly nonlinear fibers with a high SBS threshold. , 2011, , .		9
479	Selective excitation of multiple Raman Stokes wavelengths (green-yellow-red) using shaped multi-step pulses from an all-fiber PM MOPA. Optics Express, 2011, 19, 2085.	3.4	9
480	Phase regeneration of DPSK signals in a highly nonlinear lead-silicate W-type fiber. Optics Express, 2012, 20, 27419.	3.4	9
481	Phase sensitive amplification in a highly nonlinear lead-silicate fiber. Optics Express, 2012, 20, 1629.	3.4	9
482	All-Optical Processing of Multi-level Phase Shift Keyed Signals. , 2012, , .		9
483	First demonstration of a 211⁄4m few-mode TDFA for mode division multiplexing. Optics Express, 2014, 22, 10544.	3.4	9
484	Experimental Demonstration of Improved Equalization Algorithm for IM/DD Fast OFDM. IEEE Photonics Technology Letters, 2015, 27, 1780-1783.	2.5	9
485	A Tuneable Multi-Core to Single Mode Fiber Coupler. IEEE Photonics Technology Letters, 2017, 29, 591-594.	2.5	9
486	Cavity-induced phase noise suppression in a Fabry–Perot modulator-based optical frequency comb. Optics Letters, 2017, 42, 1536.	3.3	9

#	Article	IF	CITATIONS
487	Widely Tunable, Narrow-Linewidth, High-Peak-Power, Picosecond Midinfrared Optical Parametric Amplifier. IEEE Journal of Selected Topics in Quantum Electronics, 2018, 24, 1-6.	2.9	9
488	Demonstration of Single-Mode Multicore Fiber Transport Network With Crosstalk-Aware In-Service Optical Path Control. Journal of Lightwave Technology, 2018, 36, 1451-1457.	4.6	9
489	Hollow-Core NANF for High-Speed Short-Reach Transmission in the S+C+L-Bands. Journal of Lightwave Technology, 2021, 39, 6167-6174.	4.6	9
490	Controllable duration and repetition-rate picosecond pulses from a high-average-power OP-GaAs OPO. Optics Express, 2020, 28, 32540.	3.4	9
491	All-fiber acoustooptic filter with low-polarization sensitivity and no frequency shift. IEEE Photonics Technology Letters, 1997, 9, 461-463.	2.5	8
492	Detailed Comparison of Injection-Seeded and Self-Seeded Performance of a 1060-nm Gain-Switched Fabry–PÉrot Laser Diode. IEEE Journal of Quantum Electronics, 2008, 44, 645-651.	1.9	8
493	Tunable synchronously-pumped fiber Raman laser in the visible and near-infrared exploiting MOPA-generated rectangular pump pulses. Optics Letters, 2011, 36, 2050.	3.3	8
494	Suppression of Gain Variation in a PSA-Based Phase Regenerator Using an Additional Harmonic. IEEE Photonics Technology Letters, 2014, 26, 2074-2077.	2.5	8
495	Single polarization picosecond fiber MOPA power scaled to beyond 500 W. Laser Physics Letters, 2014, 11, 085103.	1.4	8
496	Data transmission through up to 74.8 km of hollow-core fiber with coherent and direct-detect transceivers. , 2015, , .		8
497	Polarization Insensitive Wavelength Conversion in a Low-Birefringence SiGe Waveguide. IEEE Photonics Technology Letters, 2016, 28, 1221-1224.	2.5	8
498	Optical Injection-Locked Directly Modulated Lasers for Dispersion Pre-Compensated Direct-Detection Transmission. Journal of Lightwave Technology, 2018, 36, 4967-4974.	4.6	8
499	Toward High Accuracy Positioning in 5G via Passive Synchronization of Base Stations Using Thermally-Insensitive Optical Fibers. IEEE Access, 2019, 7, 113197-113205.	4.2	8
500	Nondestructive measurement of the roughness of the inner surface of hollow core-photonic bandgap fibers. Optics Letters, 2016, 41, 5086.	3.3	8
501	Anti-Resonant, Mid-Infrared Silica Hollow-Core Fiber. , 2020, , .		8
502	Bacterial dimethyl sulphoxide reductases and nitrate reductases. Biochemical Society Transactions, 1991, 19, 605-608.	3.4	7
503	Demonstration of 205 km transmission of 35 GHz, 5 ps pulses generated from a diode-driven, low-jitter, beat-signal to soliton train conversion source. Electronics Letters, 1995, 31, 470-472.	1.0	7
504	Second-harmonic generation in hexagonally-poled lithium niobate slab waveguides. Electronics Letters, 2003, 39, 75.	1.0	7

#	Article	IF	CITATIONS
505	Optical interconnection of core and metro networks [Invited]. Journal of Optical Networking, 2008, 7, 928.	2.5	7
506	TDM-to-WDM conversion from 130 Gbit/s to 3 × 43 Gbit/s using XPM in a NOLM switch. , 2008, , .		7
507	Analysis of modal interference in Photonic Bandgap Fibres. , 2010, , .		7
508	Phase-regenerative wavelength conversion in periodically poled lithium niobate waveguides. Optics Express, 2011, 19, 11705.	3.4	7
509	Fiber MOPA based tunable source for terahertz spectroscopy. Laser Physics Letters, 2012, 9, 350-354.	1.4	7
510	Overcoming the Challenges of Splicing Dissimilar Diameter Solid-Core and Hollow-Core Photonic Band Gap Fibers. , 2013, , .		7
511	Robust Low Loss Splicing of Hollow Core Photonic Bandgap Fiber to Itself. , 2013, , .		7
512	Studying the limits of production rate and yield for the volume manufacturing of hollow core photonic band gap fibers. Optics Express, 2015, 23, 32179.	3.4	7
513	Discrete Multitone Format for Repeater-Less Direct-Modulation Direct-Detection Over 150 km. Journal of Lightwave Technology, 2016, 34, 3223-3229.	4.6	7
514	Current status of few mode fiber amplifiers for spatial division multiplexed transmission. Journal of Optics (India), 2016, 45, 275-284.	1.7	7
515	Demonstration of arbitrary temporal shaping of picosecond pulses in a radially polarized Yb-fiber MOPA with > 10 W average power. Optics Express, 2017, 25, 15402.	3.4	7
516	Compact chirped-pulse amplification systems based on highly Tm ³⁺ -doped germanate fiber. Optics Letters, 2021, 46, 3013.	3.3	7
517	Lowâ€Latency WDM Intensityâ€Modulation and Directâ€Detection Transmission Over >100Âkm Distances in a Hollow Core Fiber. Laser and Photonics Reviews, 2021, 15, 2100102.	8.7	7
518	Adiabatic higher-order mode microfibers based on a logarithmic index profile. Optics Express, 2020, 28, 19126.	3.4	7
519	Hollow-core fiber delivery of broadband mid-infrared light for remote spectroscopy. Optics Express, 2022, 30, 7044.	3.4	7
520	Distributed dispersion measurements and control within continuously varying dispersion tapered fibers. IEEE Photonics Technology Letters, 1997, 9, 1511-1513.	2.5	6
521	Generation, recognition and recoding of 64-chip bipolar optical code sequences using superstructured fibre Bragg gratings. Electronics Letters, 2001, 37, 190.	1.0	6
522	Performance comparison of spectrum-slicing techniques employing SOA-based noise suppression at the transmitter or receiver. IEEE Photonics Technology Letters, 2006, 18, 1494-1496.	2.5	6

#	Article	IF	CITATIONS
523	Efficient higher-order mode filtering in multimode optical fiber based on an optical microwire. , 2008, , .		6
524	In situ spatially-resolved thermal and Brillouin diagnosis of high-power ytterbium-doped fibre laser by Brillouin optical time domain analysis. Electronics Letters, 2009, 45, 153.	1.0	6
525	Full characterization and comparison of phase properties of narrow linewidth lasers operating in the C-band. Proceedings of SPIE, 2011, , .	0.8	6
526	Freely diffusing versus adsorbed protein: Which better mimics the cellular state of a redox protein?. Electrochimica Acta, 2013, 110, 73-78.	5.2	6
527	First Demonstration of a 2- <inline-formula> <tex-math notation="TeX">\$mu{m m}\$ </tex-math> </inline-formula> OTDR and Its Use in Photonic Bandgap <inline-formula> <tex-math notation="TeX">\${m CO}_{2}\$ </tex-math> </inline-formula> Sensing Fiber. IEEE Photonics Technology Letters, 2014, 26, 889-892.	2.5	6
528	Membrane-spanning electron transfer proteins from electrogenic bacteria: Production and investigation. Methods in Enzymology, 2018, 613, 257-275.	1.0	6
529	Cavity ring-down in a photonic bandgap fiber gas cell. , 2008, , .		6
530	High pulse energy fibre laser as an excitation source for photoacoustic tomography. Optics Express, 2020, 28, 34255.	3.4	6
531	Minimizing Differential Modal Gain in Cladding Pumped MM-EDFAs for Mode Division Multiplexing in C and L Bands. , 2014, , .		6
532	Simplified Impulse Response Characterization for Mode Division Multiplexed Systems. , 2016, , .		6
533	ML-Assisted Equalization for 50-Gb/s/λ O-Band CWDM Transmission Over 100-km SMF. IEEE Journal of Selected Topics in Quantum Electronics, 2022, 28, 1-10.	2.9	6
534	Frequency-resolved optical gating in the 155 Âμm band via cascaded chi^(2) processes. Journal of the Optical Society of America B: Optical Physics, 2005, 22, 1985.	2.1	5
535	Frequency-resolved optical gating in a quasi-phase-matched LiNbO/sub 3/ waveguide. IEEE Photonics Technology Letters, 2005, 17, 849-851.	2.5	5
536	Optical regeneration using self-phase modulation and quasi-continuous filtering. IEEE Photonics Technology Letters, 2006, 18, 1350-1352.	2.5	5
537	Novel fabrication method of highly-nonlinear silica holey fibres. , 2006, , .		5
538	Ultraviolet writing of channel waveguides in proton-exchanged LiNbO3. Journal of Applied Physics, 2007, 101, 014110.	2.5	5
539	Saturation effects in degenerate phase sensitive fiber optic parametric amplifiers. , 2010, , .		5
540	Multichannel Wavelength Conversion of 40-Gb/s Nonreturn-to-Zero DPSK Signals in a Lead–Silicate Fiber. IEEE Photonics Technology Letters, 2010, 22, 1153-1155.	2.5	5

#	Article	IF	CITATIONS
541	500km remote interrogation of optical sensor arrays. Proceedings of SPIE, 2011, , .	0.8	5
542	Analysis of acceptable spectral windows of quadratic cascaded nonlinear processes in a periodically poled lithium niobate waveguide. Optics Express, 2011, 19, 8327.	3.4	5
543	All fiber components for multimode SDM systems. , 2012, , .		5
544	Demonstration of Space-to-Wavelength Conversion in SDM Networks. IEEE Photonics Technology Letters, 2015, 27, 828-831.	2.5	5
545	Amplification of 12 OAM States in an Air-Core EDF. , 2015, , .		5
546	Phase regeneration of an M-PSK signal using partial regeneration of its M/2-PSK second phase harmonic. Optics Communications, 2015, 334, 35-40.	2.1	5
547	Wavelength conversion technique for optical frequency dissemination applications. Optics Letters, 2016, 41, 1716.	3.3	5
548	Optical Predistortion Enabling Phase Preservation in Optical Signal Processing Demonstrated in FWM-Based Amplitude Limiter. Journal of Lightwave Technology, 2017, 35, 963-970.	4.6	5
549	Highly efficient frequency doubling and quadrupling of a short-pulsed thulium fiber laser. Applied Physics B: Lasers and Optics, 2018, 124, 59.	2.2	5
550	Polarization Effects on Thermally Stable Latency in Hollow-Core Photonic Bandgap Fibers. Journal of Lightwave Technology, 2021, 39, 2142-2150.	4.6	5
551	Finesse Limits in Hollow Core Fiber based Fabry-Perot interferometers. Journal of Lightwave Technology, 2021, 39, 4489-4495.	4.6	5
552	Recent Breakthroughs in Hollow Core Fiber Technology. , 2021, , .		5
553	Light-induced specular-reflectivity suppression at a gallium/silica interface. Optics Letters, 2000, 25, 1594.	3.3	4
554	Structural and Functional Flexibility of Bacterial Respiromes. , 2008, , 97-128.		4
555	Multiple access interference rejection in OCDMA using a two-photon absorption based semiconductor device. Optics Communications, 2009, 282, 1281-1286.	2.1	4
556	Improved method for estimating the minimum length of modal filters fabricated for stellar interferometry. Optics Express, 2009, 17, 1935.	3.4	4
557	Optical WDM regeneration: status and future prospects. , 2009, , .		4
558	All-optical phase-regenerative multicasting of 40 Gbit/s DPSK signal in a degenerate phase sensitive amplifier. , 2010, , .		4

#	Article	IF	CITATIONS
559	Wide spectral range confocal microscope based on endlessly single-mode fiber. Optics Express, 2010, 18, 18811.	3.4	4
560	Phase locking and carrier extraction schemes for phase sensitive amplification. , 2010, , .		4
561	High performance architecture design for large scale fibre-optic sensor arrays using distributed EDFAs and hybrid TDM/DWDM. Measurement Science and Technology, 2013, 24, 094024.	2.6	4
562	Generation of mode-locked optical pulses at 1035 nm from a fiber Bragg grating stabilized semiconductor laser diode. Optics Express, 2014, 22, 13366.	3.4	4
563	Practical Considerations on Discrete Multi-tone Transmission for Cost-effective Access Networks. , 2015, , .		4
564	Multiport Fiber Optic Beam Splitters for Space Division Multiplexed (SDM) Systems. IEEE Photonics Technology Letters, 2020, 32, 795-798.	2.5	4
565	4-Level Alternate-Mark-Inversion for Reach Extension in the O-Band Spectral Region. Journal of Lightwave Technology, 2021, 39, 2847-2853.	4.6	4
566	nosX is essential for whole-cell N2O reduction in Paracoccus denitrificans but not for assembly of copper centres of nitrous oxide reductase. Microbiology (United Kingdom), 2020, 166, 909-917.	1.8	4
567	Novel Polarisation-assisted Phase Sensitive Optical Signal Processor Requiring Low Nonlinear Phase Shifts. , 2014, , .		4
568	Hollow-core fiber Fabry–Perot interferometers with reduced sensitivity to temperature. Optics Letters, 2022, 47, 2510.	3.3	4
569	High-energy, mid-IR, picosecond fiber-feedback optical parametric oscillator. Optics Letters, 2022, 47, 3600.	3.3	4
570	Nonlinearity in holey optical fibers:?measurement and future opportunities—errata. Optics Letters, 1999, 24, 1647.	3.3	3
571	Cascaded-chi(2)-interaction-based frequency-resolved optical gating in a periodically poled LiNbO3 waveguide. Optics Letters, 2006, 31, 244.	3.3	3
572	Delay-gain decoupling in Brillouin-assisted slow light. Optics Letters, 2007, 32, 2701.	3.3	3
573	Distributed-Phase OCDMA Encoder–Decoders Based on Fiber Bragg Gratings. IEEE Photonics Technology Letters, 2007, 19, 574-576.	2.5	3
574	Low Walk-Off Kerr-Shutter Using a Dispersion-Shifted Lead Silicate Holey Fiber. IEEE Photonics Technology Letters, 2007, 19, 1112-1114.	2.5	3
575	Developing Single-Mode Tellurite Glass Holey Fiber for Infrared Nonlinear Applications. Advances in Science and Technology, 0, , .	0.2	3
576	Over 55W of frequency doubled light at 530 nm pumped by an all-fiber diffraction limited picosecond fibre MOPA. , 2010, , .		3

#	Article	IF	CITATIONS
577	Use of a pulsed fibre laser as an excitation source for photoacoustic tomography. Proceedings of SPIE, 2011, , .	0.8	3
578	Mode division multiplexing over 19â€cell hollowâ€core photonic bandgap fibre by employing integrated mode multiplexer. Electronics Letters, 2014, 50, 1227-1229.	1.0	3
579	Compact picosecond mid-IR PPLN OPO with controllable peak powers. OSA Continuum, 2020, 3, 2741.	1.8	3
580	Widely Tunable Actively Mode-Locked Bi-Doped Fiber Laser Operating in the O-Band. IEEE Photonics Technology Letters, 2022, 34, 711-714.	2.5	3
581	Structural and optical characterisation of holey fibres using scanning probe microscopy. Electronics Letters, 2001, 37, 1283.	1.0	2
582	A Reconfigurable Optical Header Recognition System for Optical Packet Routing Applications. IEEE Photonics Technology Letters, 2006, 18, 2395-2397.	2.5	2
583	Fibre Bragg Grating Based Continuous-Phase Encoder-Decoders for OCDMA Networks. , 2006, , .		2
584	2R regeneration architectures based on multi-segmented fibres. , 2008, , .		2
585	Externally modulated diode-seeded Yb3+-doped fiber MOPA pumped high power optical parametric oscillator. , 2009, , .		2
586	Supercontinuum generation and nonlinearity in soft glass fibres. , 0, , 82-118.		2
587	Elimination of the chirp of optical pulses through cascaded nonlinearities in periodically poled lithium niobate waveguides. Optics Letters, 2010, 35, 3724.	3.3	2
588	Generation of ultra-high repetition rate pulses in a highly nonlinear dispersion-tailored compound glass fibre. , 2010, , .		2
589	Phase sensitive amplifiers for regeneration of phase encoded optical signal formats. , 2011, , .		2
590	Robust optical injection locking to a 250 MHz frequency comb without narrow-band optical pre-filtering. , 2011, , .		2
591	Bend sensors based on periodically tapered soft glass fibers. , 2011, , .		2
592	Pulse shaping-assisted nonlinear spectral broadening. , 2011, , .		2
593	All-Optical Regeneration of Phase Encoded Signals. , 2013, , 589-639.		2
594	Highly Nonlinear Tellurite Glass Fiber for Broadband Applications. , 2014, , .		2

#	Article	IF	CITATIONS
595	Analysis and comparison of intermodal coupling coefficient of standard and hollow core few moded fibres. , 2015, , .		2
596	Real-Time Modal Analysis via Wavelength- Swept Spatial and Spectral (S ²) Imaging. IEEE Photonics Technology Letters, 2016, , 1-1.	2.5	2
597	Exploring nonlinear pulse propagation, Raman frequency conversion and near octave spanning supercontinuum generation in atmospheric air-filled hollow-core Kagomé fiber. Proceedings of SPIE, 2017, , .	0.8	2
598	Long Length Fibre Fabry-Perot Interferometers and their Applications in Fibre Characterization and Temperature Sensing. , 2019, , .		2
599	Temperature-insensitive delay-line fiber interferometer. , 2021, , .		2
600	Hollow core fiber temperature sensitivity reduction via winding on a thermally-insensitive coil. , 2021, , .		2
601	Assorted core air-clad fibre. Electronics Letters, 2000, 36, 2065.	1.0	2
602	Flat, Broadband Supercontinuum Generation at Low Pulse Energies in a Dispersion-Tailored Lead-Silicate Fibre. , 2011, , .		2
603	Feed-Forward Optical Domain Carrier Recovery from High Baud Rate PSK Signals using Relatively Slow Electronics. , 2011, , .		2
604	Multichannel Wavelength Conversion of 40Gbit/s NRZ DPSK Signals in a Highly Nonlinear Dispersion Flattened Lead Silicate Fibre. , 2010, , .		2
605	Soft Glass Based Large Mode Area Photonic Bandgap Fibre for Mid-Infrared Applications. , 2011, , .		2
606	Accurate Loss and Surface Mode Modeling in Fabricated Hollow-Core Photonic Bandgap Fibers. , 2014, , ,		2
607	Optical Injection Locking for Carrier Phase Recovery and Regeneration. , 2017, , .		2
608	High fidelity femotosecond pulses from an ultrafast fiber laser system via adaptive amplitude and phase pre-shaping. , 2009, , .		2
609	Robust design of all-optical PSK regenerator based on phase sensitive amplification. , 2011, , .		2
610	Phase Noise and Jitter Characterization of Pulses Generated by Optical Injection Locking to an Optical Frequency Comb. , 2012, , .		2
611	<title>Switching and passive mode-locking of fiber lasers using nonlinear loop mirrors (Invited) Tj ETQq1 1 0.784</td><td>314 rgBT</td><td>/Oyerlock 10</td></tr><tr><td>612</td><td>Optical Regeneration. Springer Series in Optical Sciences, 2015, , 129-155.</td><td>0.7</td><td>2</td></tr></tbody></table></title>		

#	Article	IF	CITATIONS
613	Radially polarized Yb-fiber MOPA producing 10 W output using SLM based pulse shaping for efficient generation of arbitrary shaped picosecond pulses. , 2016, , .		2
614	Virtual Draw of Tubular Hollow-Core Fibers. , 2018, , .		2
615	Comparative Investigations between SSMF and Hollow-core NANF for Transmission in the S+C+L-bands. , 2020, , .		2
616	Growth of Ammonium Chloride on Cleaved End-Facets of Hollow Core Fibers. , 2020, , .		2
617	Hollow core fiber Fabry-Perot interferometers with finesse over 3000. , 2020, , .		2
618	Transmission of 61 C-band Channels with L-band Interferers over Record 618km of Hollow-Core-Fiber. , 2020, , .		2
619	Introduction to the issue on novel and specialty fibers. IEEE Journal of Selected Topics in Quantum Electronics, 2001, 7, 401-402.	2.9	1
620	Opportunities in high-power fiber lasers. , 2006, , .		1
621	Processing Ultrafast Optical Signals in Broadband Telecom Systems by means of Cascaded Quadratic Nonlinearities. , 2006, , .		1
622	Parabolic Pulse Generation through Passive Reshaping of Gaussian Pulses in a Normally Dispersive Fiber. , 2007, , .		1
623	Comment on the reported fiber attenuations in the visible regime in "Fabrication of glass photonic crystal fibers with a die-cast process†Applied Optics, 2008, 47, 5078.	2.1	1
624	Applications of superstructured fibre Bragg gratings in all-optical signal processing. , 2009, , .		1
625	Control of modal properties and modal effects in air guiding photonic bandgap fibres. , 2009, , .		1
626	Visible and mid-IR output using a fibre laser pump source. , 2009, , .		1
627	Applications of highly nonlinear dispersion tailored lead silicate fibres for high speed optical communications. , 2010, , .		1
628	All-optical regeneration based on phase sensitive amplification. , 2011, , .		1
629	A fiber based synchronously pumped tunable Raman laser in the NIR. , 2011, , .		1
630	High performance fibre-optic acoustic sensor array using a distributed EDFA and hybrid TDM/DWDM, scalable to 4096 sensors. Proceedings of SPIE, 2012, , .	0.8	1

#	Article	IF	CITATIONS
631	Phase noise characterization of injection locked semiconductor lasers to a 250 MHz optical frequency comb. , 2012, , .		1
632	Coherent optical OFDM based on direct modulation of injection-locked Fabry-Perot lasers. , 2014, , .		1
633	High sensitivity gas detection using Hollow Core Photonic Bandgap Fibres designed for mid-IR operation. , 2014, , .		1
634	Novel fluid dynamics model to predict draw of hollow core photonic band-gap fibres. , 2014, , .		1
635	Cavity effect on phase noise of Fabry-Perot modulator-based optical frequency comb. , 2016, , .		1
636	Pulse energy packing effects on material transport during laser processing of \$\$<1 1 1>\$\$ < 1 1 1 > silicon. Applied Physics A: Materials Science and Processing, 2018, 124, 1.	2.3	1
637	Fully integrated SDM amplifiers. , 2018, , .		1
638	Ultralow thermal sensitivity of phase and propagation delay in hollow-core fibers. , 2018, , .		1
639	Optical Amplifiers for Mode Division Multiplexing. , 2018, , 1-25.		1
640	Spectral Difference Interferometry for the Characterization of Optical Media. Laser and Photonics Reviews, 2019, 13, 1900007.	8.7	1
641	Nonlinear control of coherent absorption and its optical signal processing applications. APL Photonics, 2019, 4, 106109.	5.7	1
642	Bi-doped fiber amplifiers for ultra-wideband optical communication systems. , 2021, , .		1
643	2-μm-band Coherent Transmission of Nyquist-WDM 16-QAM Signal by On-chip Spectral Translation. , 2021, , .		1
644	All-Optical broadband phase noise emulation. , 2012, , .		1
645	Phase Sensitive Amplification in a Highly Nonlinear Lead-Silicate Fibre. , 2011, , .		1
646	Phase-Sensitive Wavelength Conversion Based on Cascaded Quadratic Processes in Periodically Poled Lithium Niobate Waveguides. , 2011, , .		1
647	Broadband single-mode microfiber coupler for OCT. , 2009, , .		1
648	Recent Advances in Microstructured Fibers for Power Delivery. , 2009, , .		1

Recent Advances in Microstructured Fibers for Power Delivery. , 2009, , . 648

#	Article	IF	CITATIONS
649	Field-trial of an all-optical PSK regenerator in a 40 Gbit/s, 38 channel DWDM transmission experiment. , 2011, , .		1
650	Homodyne Operation of a Phase-only Optical Amplifier. , 2012, , .		1
651	Practical issues and some lessons learned from realization of phase sensitive parametric regenerators. , 2012, , .		1
652	Accurate Modelling of Hollow Core Photonic Bandgap Fibre. , 2014, , .		1
653	Inspection of Defect-Induced Mode Coupling in Hollow-Core Photonic Bandgap Fibers Using Time-of-Flight. , 2015, , .		1
654	InP-based Comb-locked Optical Super Channel Transmitter. , 2016, , .		1
655	Generation and Coherent Detection of 2-µm-band WDM-QPSK Signals by On-chip Spectral Translation. , 2020, , .		1
656	100 Gbit/s PAM-16 Transmission in the 2-µm Band over a 1.15-km Hollow-Core Fiber. , 2021, , .		1
657	Ultra-wideband IM/DD Transmission over Hollow-core Fibres. , 2021, , .		1
658	Broadband Mode Scramblers for Few-Mode Fibers Based on 3D Printed Mechanically Induced Long-Period Fiber Gratings. IEEE Photonics Technology Letters, 2022, 34, 169-172.	2.5	1
659	Comparison between the Optical Performance of Photonic Bandgap and Antiresonant Hollow Core Fibers after Long-Term Exposure to the Atmosphere. , 2022, , .		1
660	Advances in holey fibers. , 2003, , .		0
661	Parabolic pulse evolution in normally dispersive fiber amplifiers preceding the similariton formation regime. , 2006, , .		Ο
662	RGB generation by four-wave mixing in small-core holey fibers. Proceedings of SPIE, 2007, , .	0.8	0
663	Filtered optical frequency comb generator as a stable and tunable short pulse source. , 2008, , .		Ο
664	Applications of Pulse Shaping in High Power Fiber Laser Systems. , 2008, , .		0
665	Applications of Superstructured Fibre Bragg gratings in optical switching devices. , 2008, , .		0
666	Advanced fibre designs for high power laser beam delivery and generation. , 2009, , .		0

#	Article	IF	CITATIONS
667	Selective excitation of the fundamental mode in a multimode fiber using an adiabatically tapered splice. , 2009, , .		0
668	Generation of parabolic pulses and applications for optical telecommunications. , 2009, , .		0
669	100W, single mode, single polarization, picosecond, ytterbium doped fibre MOPA frequency doubled to 530nm. , 2009, , .		0
670	Parabolic Pulse Formation and Applications. , 2009, , .		0
671	Fluid-filled microstructured optical fibers and switching applications. Proceedings of SPIE, 2009, , .	0.8	0
672	Excitation of individual Raman Stokes lines of up-to ninth order using rectangular shaped optical pulses at 530 nm. , 2010, , .		0
673	A Picosecond Optical Parametric Oscillator Synchronously Pumped by an Amplified Gain-Switched Laser Diode. , 2010, , .		Ο
674	SINGLE MODE ERBIUM YTTERBIUM-DOPED FIBER LASER WITH MULTIMODE PUMPING. Journal of Nonlinear Optical Physics and Materials, 2010, 19, 203-208.	1.8	0
675	Elimination of the chirp of optical pulses through cascaded nonlinearities in periodically poled lithium niobate waveguides. , 2010, , .		Ο
676	High-Power Supercontinuum generation with picosecond pulses. , 2010, , .		0
677	Recent advances in highly nonlinear microstructured optical fibers for telecom applications. Proceedings of SPIE, 2010, , .	0.8	Ο
678	Efficient near-infrared supercontinuum generation in tellurite holey fiber pumped 320nm within the normal dispersion regime. , 2010, , .		0
679	Processing of telecommunication signals using periodically poled lithium niobate waveguides. , 2010, , \cdot		Ο
680	Phase regeneration of optical signals. , 2011, , .		0
681	Rapidly tunable, wavelength agile, visible fiber based light source exploiting Raman scattering of multi-step pulses. , 2011, , .		0
682	Simultaneous excitation of selective multiple Raman Stokes wavelengths (green-yellow-red) using shaped multi-step pulses from an all-fiber MOPA system. Proceedings of SPIE, 2011, , .	0.8	0
683	Phase sensitive parametric mixers for coherent all-optical signal processing. , 2011, , .		Ο
684	Nonlinear fibre design for broadband phase sensitive amplification. , 2011, , .		0

#	Article	IF	CITATIONS
685	Potential and practical implementations of phase sensitive amplifiers for all-optical signal regeneration. , 2011, , .		Ο
686	High power high repetition rate picosecond optical parametric oscillator pumped by frequency doubled all-fiber Yb-doped MOPA. Proceedings of SPIE, 2012, , .	0.8	0
687	An all-fiber PM MOPA pumped high-power OPO at 3.82 $\hat{1}$ 4m based on large aperture PPMgLN. , 2012, , .		Ο
688	Packet compression of complex modulation formats based on coherent optical superposition. , 2012, , .		0
689	Microstructured cladding elements to enhance the performance of large mode area leakage channel fibers. Proceedings of SPIE, 2013, , .	0.8	Ο
690	Generation of transfonn-limited picosecond pulses at 1.0 µm from a gain switched semiconductor laser diode. , 2013, , .		0
691	Stable 100 GHz pulses generated by injection locking of multiple lasers to an optical frequency comb. , 2013, , .		0
692	High-resolution broadly-tunable MOPA-based terahertz spectrometer to non-destructively probe and modulate protein electrodynamics. , 2013, , .		0
693	Signal Regeneration Techniques for Advanced Modulation Formats. , 2013, , .		0
694	Chirp reduction and on/off contrast enhancement via optical injection locking and coherent carrier manipulation. Proceedings of SPIE, 2013, , .	0.8	0
695	Demonstration of 90° optical hybrid at 2 μm wavelength range based on 4×4 MMI using diluted waveguide. , 2014, , .		0
696	Introduction: ECOC 2013 in London. Optics Express, 2014, 22, 1918.	3.4	0
697	Recent progress in SDM amplifiers. Proceedings of SPIE, 2017, , .	0.8	0
698	Data transmissions at 1.98 ŵm in cm-long SiGe waveguides. , 2017, , .		0
699	Interconnecting hollow-core fibers. , 2021, , .		Ο
700	Advanced Fibre Grating Technologies for Application in Next Generation Lasers and Networks. , 2009, ,		0
701	High pulse energy, picosecond MgO:PPLN optical parametric oscillator using a single-mode fiber for signal feedback. , 2011, , .		Ο
702	Synchronously pumped tunable Raman laser in the visible pumped by an all-fiber PM MOPA at 1060 nm. , 2011, , .		0

#	Article	IF	CITATIONS
703	All-optical regeneration based on phase sensitive amplification. , 2011, , .		0
704	160-to-40Gibt/s Time Demultiplexing in a low dispersion Lead-Silicate W-Index Profile Fiber. , 2011, , .		0
705	Field-trial of an all-optical PSK regenerator in a 40 Gbit/s, 38 channel DWDM transmission experiment. , 2011, , .		0
706	Fiber Optical Parametric Amplification of Optical Combs for Enhanced Performance and Functionality. , 2011, , .		0
707	Temporal Multiplexing of Complex Modulation Formats Facilitated by their Coherent Optical Superposition. , 2012, , .		0
708	High-energy, in-band, cladding-pumped erbium doped pulsed fiber lasers. , 2012, , .		0
709	Mid-IR coherent supercontinuum generation in all-solid step-index soft glass fibers. , 2012, , .		0
710	Analysis of Light Scattering from Surface Roughness in Hollow-Core Photonic Bandgap Fibers. , 2012, ,		0
711	Dissemination of an optical frequency comb over fiber with 3 $ ilde{A}-$ 10 $ ilde{a}^{\prime}$ 18 fractional accuracy. , 2012, , .		0
712	200W Gain-Switched-Diode-Seeded, Single-Polarization, Narrow-Linewidth, All-Fiber, Picosecond MOPA. , 2013, , .		0
713	Transmission Performance of Phase-Preserving Amplitude Regenerator based on Optical Injection Locking. , 2013, , .		0
714	Impact of Structural Distortions on the Loss Properties of Hollow-Core Photonic Bandgap Fibers. , 2013, , .		0
715	Hollow Core Fiber Technology for Data Transmission. , 2014, , .		0
716	Idler-Resonant Femtosecond Optical Parametric Oscillator with High Mid-Infra-Red Beam Quality. , 2014, , .		0
717	Optical Injection Locking based Carrier Recovery for Coherent Signal Reception. , 2015, , .		0
718	FWM-based Amplitude Limiter Realizing Phase Preservation through Cancellation of SPM Distortions. , 2016, , .		0
719	Applications of nonlinear parametric effects for advanced processing of optical signals. , 2016, , .		0
720	Multi-channel all-optical signal processing based on parametric effects. , 2016, , .		0

#	Article	IF	CITATIONS
721	Roughness measurements inside hollow glass fibers. , 2016, , .		0
722	Optical Amplifiers for Mode Division Multiplexing. , 2019, , 849-873.		0
723	Highly-Tm3+ doped Hexagonal Clad Germanate Fiber and associated CPA system for 2 µm Pulsed Fiber Lasers and Amplifiers. , 2020, , .		0
724	Amplified O-band direct-detection transmission using bismuth-doped fiber amplifiers. , 2021, , .		0
725	Generation and heterodyne detection of a 2-μm-band 16-QAM signal based on inter-band wavelength conversion. , 2020, , .		0
726	Compact picosecond mid-IR PPLN OPO in burst-mode operation. EPJ Web of Conferences, 2020, 243, 18004.	0.3	0
727	Transmission Of Frequency Comb Over 7.7 km Of Hollow Core Fiber. , 2021, , .		0
728	Experimental Demonstration of 50-Gb/s/Z O-band CWDM Direct-Detection Transmission over 100-km SMF. , 2021, , .		0
729	High-energy, mid-IR, picosecond fiber-feedback OPO. , 2021, , .		0
730	Polarization Stable Hollow Core Fiber Interferometer With Faraday Rotator Mirrors. IEEE Photonics Technology Letters, 2021, 33, 1503-1506.	2.5	0